Mon. Not. R. astr. Soc. (1976) **174**, 345–391.

THE RECOMBINATION AND LEVEL POPULATIONS OF IONS—I

Hydrogen and Hydrogenic Ions

Alan Burgess and Hugh P. Summers

Department of Applied Mathematics and Theoretical Physics, University of Cambridge, Cambridge

(Received 1975 July 28; in original form 1974 August 21)

SUMMARY

A description is given of the atomic processes occurring in an unbounded plasma containing ions, electrons and protons and permeated by external radiation fields. The ionization equilibrium is formulated in a matrix scheme which simplifies the definition of the effective recombination and ionization rate coefficients, namely the 'collisional radiative coefficients', and also permits the unification of statistical and mechanistic approaches to recombination. A method of numerical solution of the statistical balance equations for the collisional radiative coefficients and the level populations (including the very highly-excited levels) is given. Results are presented for hydrogen and hydrogenic ions in both graphical and numerical form. The collisional radiative recombination and ionization coefficients are given for hydrogen and hydrogenic ions over wide ranges of electron density and temperature. The influence of radiation and free particle temperature and density on the excited level populations of hydrogen is demonstrated. Tabulations of level populations are given appropriate to H I regions and to fairly dense H II regions. Simple expressions for bound–bound and bound–free Gaunt factors and for impact parameter cross-sections are given as Appendices.

1. INTRODUCTION

The study of populations of highly-excited states of ions in a plasma in which electrons and ions are recombining is of considerable importance, both because of interest in the absorption and emission spectrum and because of their influence on effective recombination and ionization rates. A substantial amount of recombination can take place through excited states both in high density plasmas and (when the dielectronic process is active, Burgess (1964a)) in low density astrophysical plasmas. The ions readily experience transitions between highly-excited states in the presence of free particles and radiation. This both complicates the calculation of the populations of the excited states and causes the populations and the effective recombination and ionization rates to be sensitive in many circumstances to free particle and radiation density and temperature (Burgess & Summers 1969).

The present paper is concerned with the examination of these influences on the recombination of hydrogenic ions (i.e. of nuclei and electrons) and on the population structure of hydrogen. The subject has been investigated by a number of authors. Recombination at high electron densities has been considered approximately by Hinnov & Hirschberg (1962), by D'Angelo (1961, 1965) and at high and intermediate densities more completely by Bates, Kingston & McWhirter (1962),

referred to hereafter as BKMcW. A number of approximate treatments of varying reliability of the excited state population structure have been performed (Seaton 1964; Hoang-Binh 1968; Dyson 1969; Sejnowski & Hjellming 1969; Dupree 1972).

A matrix condensation method for treating the problem has been developed by the present authors and a summary of it is given in Burgess & Summers (1969). Brocklehurst (1970, 1971, 1973) has published some detailed results obtained using the method. It is the purpose of the present paper to give details and discussion of the method and to present some further results relating to a wide range of conditions of free particle and radiation density and temperature. Situations from high density laboratory plasmas to the interstellar atomic hydrogen gas can be described. The methods to be developed apply generally to any ion except that dielectronic recombination and other processes involving inner shells such as autoionization are not included. This is the subject of a separate paper (Burgess & Summers, to be published).

In Section 2, the relevant reactions which take place in an unbounded plasma are mentioned. The equations for statistical equilibrium in the plasma can be formulated in a general matrix scheme which clarifies the definitions of effective recombination and ionization rates and enables the connection between statistical and mechanistic approaches to recombination to be unified. This is considered in Section 3. Details of the mathematical description of the atomic processes is given in Section 4 and of the numerical solution in Section 5. Collisional radiative recombination of hydrogen and hydrogenic ions is studied in Section 6 while in Section 7 population structure of hydrogen in astrophysical plasmas is considered in detail.

Some of the intermediate formulae obtained in this calculation, such as simple expressions for collision cross-sections, bound–bound and bound–free Gaunt factors have not previously received wide circulation. These may be of value to other workers.

2. REACTIONS IN A RECOMBINING PLASMA

Under most circumstances of interest here, the plasma forms an open system, in general far from thermodynamic equilibrium. Radiation is lost from the plasma, and energy is injected into it from external sources both as radiation and as thermal kinetic energy of the free particles. The time development or equilibrium of the populations of the ions in such as plasma is described by statistical balance. Consequently detailed knowledge must be obtained of all the relevant individual reactions occurring in the plasma. Since large scale dynamical and interactive effects are not the subject of this work, it is assumed that the external conditions can be specified locally.

Let $X^{+(z)}(i)$ be a z-times ionized atom in the state i and $X^{+(z-1)}(i, nl)$ be a $(z-1)$-times ionized atom with parent configuration i and a further electron in the nl shell. Since dielectronic recombination and other inner shell processes are not considered here, the state i remains unchanged throughout the recombination of $X^{+(z)}$. For hydrogenic ions, i is just the state corresponding to the bare nucleus. In the interaction of $X^{+(z-1)}(i, nl)$ with the radiation field, the following bound–bound radiative processes occur.

$$X^{+(z-1)}(i, nl) \rightleftarrows X^{+(z-1)}(i, n'l') + h\nu \tag{1}$$

$$X^{+(z-1)}(i, nl) + h\nu \rightarrow X^{+(z-1)}(i, n'l') + h\nu + h\nu. \tag{2}$$

The forward reaction in (1) is the process of spontaneous emission. The reverse reaction in (1) and reaction (2) are the processes of photoexcitation and stimulated emission respectively, induced by the radiation field. It is assumed that the plasma is optically thin in its own emitted radiation so that these reactions are induced by the external radiation field. The external radiation field in an astrophysical context might be typically that due to stellar radiation in a gaseous nebula or the 3 K universal background radiation or the photospheric radiation of the Sun in the chromosphere and corona. It can therefore be adequately described by diluted blackbody radiation at some temperature T_r and dilution W or by a superposition of such radiation fields. The radiation field appropriate to transitions involving the lowest level of an ion however may require modification. For example in an optically thick hydrogen nebula, radiation in the Lyman continuum is strongly attenuated, while Lyman α radiation is contained and so builds up to high intensities. Hence the effective dilution factors of the radiation coupling to the ground state may have to be specified separately from the general dilution of the external radiation field to make allowance for this.

The corresponding bound–free radiative processes are

$$X^{+(z)}(i) + e(E'l') \rightleftarrows X^{+(z-1)}(i, nl) + h\nu \tag{3}$$

$$X^{+(z)}(i) + e(E'l') + h\nu \rightarrow X^{+(z-1)}(i, nl) + h\nu + h\nu. \tag{4}$$

The forward reaction in (3) is radiative recombination, a free electron of energy E' and angular momentum quantum number l' recombining to the excited state nl of the parent ion $X^{+(z)}(i)$. The reverse reaction in (3) and reaction (4) are the processes of photoionization and stimulated recombination respectively. When no external radiation field is present, only the forward reactions in (1) and (3) occur.

Bound–bound transitions are also induced by collisions with free particles. The processes of collisional excitation and de-excitation by electrons are

$$X^{+(z-1)}(i, nl) + e(E''l'') \rightleftarrows X^{+(z-1)}(i, n'l') + e(E'''l'''). \tag{5}$$

Since the cross-sections for Coulomb scattering of free electrons with each other are very large, energy is redistributed rapidly amongst them. It can therefore be assumed to high accuracy that the free electrons are thermalized, having a maxwellian distribution at some temperature T_e. The largest cross-sections in (5) are those for which $n = n'$ and $l = l' \pm 1$ since they are zero energy difference transitions of long-range dipole type. The cross-sections for such collisions in hydrogen have been calculated by Pengelly & Seaton (1964) using the fact that the target states have only finite radiative lifetimes. Their results show that the cross-sections are so large for values of electron density and n of relevance here that it is a very good approximation to assume statistical relative populations for the l-states. This is also true for hydrogenic ions to which their results apply with only a small correction.

Mention has so far only been made of electron collisions in causing transitions between excited states. Consideration must also be given to other free particles which may be present. Neutral particles interact much less strongly than charged particles and may be neglected. In any real astrophysical plasma the abundances of elements other than hydrogen are low and so protons and possibly helium ions (which can be treated similarly) are the only other free particles which need to be

considered. For transitions of moderate energy difference relative to the mean kinetic energy of the free particles, electron collision cross-sections are larger than proton collision cross-sections. However, as the energy difference becomes small, the position is reversed and, for example in transitions of zero energy difference as described above, protons are more efficient than electrons. Therefore cognizance must also be taken of proton collisions in inducing transitions between neighbouring highly-excited states. These reactions are

$$X^{+(z-1)}(i, nl)+p \rightleftarrows X^{+(z-1)}(i, n'l')+p \tag{6}$$

for $\Delta n = |n-n'|$ small. As for the free electrons, it is assumed that the protons have some maxwellian distribution at a temperature $T_{\rm p}$ which may be different from the electron temperature $T_{\rm e}$ because the redistribution of kinetic energy between electrons and protons may be slower than between protons themselves and electrons themselves.

The corresponding bound–free processes of electron collisional ionization and three-body recombination are

$$X^{+(z)}(i)+e(E'l')+e(E''l'') \rightleftarrows X^{+(z-1)}(i, nl)+e(E'''l'''). \tag{7}$$

Assembling all these processes tending to populate and depopulate levels, the equations for the time dependence of the level populations are obtained.

$$\begin{aligned}
&\sum_{n'>n}[A_{n'\to n}+u(\nu)\,B_{n'\to n}+N_{\rm e}q_{n'\to n}{}^{\rm e}+N_{\rm p}q_{n'\to n}{}^{\rm p}]\,N_{n'}\\
&\qquad+\sum_{n''<n}[u(\nu)\,B_{n''\to n}+N_{\rm e}q_{n''\to n}{}^{\rm e}+N_{\rm p}q_{n''\to n}{}^{\rm p}]\,N_{n''}\\
&\qquad+N_{\rm e}N_{+}\alpha_n{}^{r}+N_{\rm e}{}^{2}N_{+}\alpha_n{}^{3}+N_{\rm e}N_{+}\int u(\nu)\,B_{\kappa\to n}\,d\kappa\\
&=\Big\{\sum_{n'>n}[u(\nu)\,B_{n\to n'}+N_{\rm e}q_{n\to n'}{}^{\rm e}+N_{\rm p}q_{n\to n'}{}^{\rm p}]\\
&\qquad+\sum_{n''<n}[A_{n\to n''}+u(\nu)\,B_{n\to n''}+N_{\rm e}q_{n\to n''}{}^{\rm e}+N_{\rm p}q_{n\to n''}{}^{\rm p}]\\
&\qquad+\int u(\nu)\,B_{n\to\kappa}\,d\kappa+N_{\rm e}q_{n\to\epsilon}\Big\}\,N_n+\frac{dN_n}{dt}.
\end{aligned} \tag{8}$$

N_n is the population of the state $X^{+(z-1)}(i, n)$ and N_+ of the parent ion $X^{+(z)}(i)$. $N_{\rm e}$ is the free electron density and $N_{\rm p}$ the free proton density. A and B are the usual Einstein coefficients, $q^{\rm e}$ and $q^{\rm p}$ denote collisional rates due to electrons and protons,

$$\int u(\nu)\,B_{n\to\kappa}\,d\kappa$$

and

$$\int u(\nu)\,B_{\kappa\to n}\,d\kappa$$

denote photoionization and stimulated recombination, $q_{n\to\epsilon}$ is the collisional ionization rate, $\alpha_n{}^{r}$ and $\alpha_n{}^{3}$ denote radiative and three-body recombination and $u(\nu)$ is the energy density of the radiation field. There is one such equation for each value of n, n spanning over all levels from the ground level n_0 to ∞. n_0 is the effective ground level and may of course correspond to principal quantum number other than 1. For example in case B of Baker & Menzel (1938) $n_0 = 2$.

3. MATRIX DESCRIPTION

It is informative to examine equations (8) in the first instance from a general viewpoint. Using index notation and summation convention, let $\mathscr{A}_{ij}$, $\mathscr{R}_{ij}$ and $\mathscr{Q}_{ij}$, $(i \neq j)$ be the rate coefficients from level i to level j due to spontaneous, induced radiative and collisional processes respectively, and let $\mathscr{A}_{ii}$, $\mathscr{R}_{ii}$ and $\mathscr{Q}_{ii}$ be the corresponding total loss rate coefficients from level i. Also let $N_e N_+ r_i$ be the recombination rate to the level i directly from the continuum. It is convenient to write this in terms of a two-body process. It does not imply neglect of three-body recombination. Then equations (8) become

$$(\mathscr{A}_{ij}+\mathscr{R}_{ij}+\mathscr{Q}_{ij})\, N_j = N_e N_+ r_i - \frac{dN_i}{dt}$$

or more simply putting $C_{ij} = \mathscr{A}_{ij}+\mathscr{R}_{ij}+\mathscr{Q}_{ij}$

$$C_{ij}N_j = N_e N_+ r_i - \frac{dN_i}{dt} \tag{9}$$

where C_{ij} describes all the collisional and radiative processes linking levels i and j and C_{ii} is the total loss rate coefficient from the level i. In statistical equilibrium these equations reduce to

$$C_{ij}N_j^{eq} = N_e N_+ r_i \tag{10}$$

where N_j^{eq} are the equilibrium populations of the levels of the ions.

3.1 *Collisional radiative recombination and ionization coefficients*

From equations (9) it is not immediately obvious what the effective recombination and ionization rates are, since for example an electron recombining on to an excited level may be re-ejected into the continuum without ever reaching the ground level, while an electron may pass through the ground level several times without entering the continuum. However, from a consideration of the relaxation times (see Section 3.3 below) of the excited states a meaningful definition of effective recombination and ionization rates can be given. As discussed by BKMcW, except at very high densities the relaxation of the excited levels is very much more rapid than that of the ground level. Thus the excited states reach an equilibrium very rapidly relative to the ground level at each moment of time. Equations (9) can therefore be replaced by the set

$$\begin{aligned} C_{1j}N_j &= N_e N_+ r_1 - \frac{dN_1}{dt} \\ C_{ij}N_j &= N_e N_+ r_i, \quad (i \neq 1). \end{aligned} \tag{11}$$

This then yields

$$(C_{11} - \bar{C}_{1j}\bar{C}_{jk}^{-1}\bar{C}_{k1})\, N_1 = N_e N_+ (r_1 - \bar{C}_{1j}\bar{C}_{jk}^{-1} r_k) - \frac{dN_1}{dt} \tag{12}$$

where $\bar{}$ denotes that the summation index does not take the value 1. *On the basis of this equation, an overall ionization coefficient S_{cr} and recombination coefficient α_{cr} can be defined, the ' collisional–radiative ' coefficients of BKMcW,

$$\alpha_{cr} = r_1 - \bar{C}_{1j}\bar{C}_{jk}^{-1} r_k \tag{13}$$

$$S_{cr} = (C_{11} - \bar{C}_{1j}\bar{C}_{jk}^{-1}\bar{C}_{k1})/N_e. \tag{14}$$

* The order of the operations of inversion, specification of index values and limitation of range of index values (where appropriate) is exemplified by $\bar{C}_{jk}^{-1} \equiv ((\bar{C})^{-1})_{jk}$.

These coefficients can be obtained in the convenient form

$$\alpha_{\rm cr} = N_1^{\rm eq}/N_{\rm e}N_+[C^{-1}]_{11} \tag{15}$$

$$S_{\rm cr} = 1/N_{\rm e}[C^{-1}]_{11}, \tag{16}$$

where $N_1^{\rm eq}$ is the solution of the equilibrium equations (10),

$$N_1^{\rm eq} = N_{\rm e}N_+C_{1i}^{-1}r_i. \tag{17}$$

Note that

$$\frac{N_1}{[C^{-1}]_{11}} = \frac{N_1^{\rm eq}}{[C^{-1}]_{11}} - \frac{dN_1}{dt}. \tag{18}$$

This method can be generalized to the case of several metastable levels with long relaxation times. In the following expressions, Greek suffices are used to denote metastable levels, which are supposed without loss of generality to occupy the first m levels, and roman suffices for all other levels. The use of these suffices implies choosing the submatrices corresponding to the allowed values of the suffices prior to matrix operations such as inversion. The extension of equations (11) is

$$\begin{aligned} C_{\rho\sigma}N_\sigma + C_{\rho j}N_j &= N_{\rm e}N_+r_\rho - \frac{dN_\rho}{dt} \qquad 1 \le \rho \le m \\ C_{ij}N_j + C_{i\sigma}N_\sigma &= N_{\rm e}N_+r_i \qquad\qquad i > m \end{aligned} \tag{19}$$

and so

$$(C_{\rho\sigma} - C_{\rho j}C_{ji}^{-1}C_{i\sigma})\,N_\sigma = N_{\rm e}N_+(r_\rho - C_{\rho j}C_{ji}^{-1}r_i) - \frac{dN_\rho}{dt}. \tag{20}$$

Let A be the inverse of the complete C matrix. Then the time-dependence of the metastable levels becomes

$$A_{\rho\sigma}^{-1}N_\sigma = N_{\rm e}N_+R_\rho - \frac{dN_\rho}{dt} \tag{21}$$

where

$$R_\rho = A_{\rho\sigma}^{-1}N_\sigma^{\rm eq}/N_{\rm e}N_+.$$

When all the levels are assumed to be metastable this just reduces to the original complete set of rate equations (9) and when only the ground level is metastable to equation (18) as expected. R_ρ is the generalized collisional radiative recombination coefficient to the level ρ and $A_{\rho\rho}^{-1}/N_{\rm e}$ the generalized total loss rate coefficient from level ρ. The $A_{\rho\sigma}$ $(\rho \neq \sigma)$ are generalized coefficients for transitions between the metastable levels.

It is convenient to mention at this point that the application of a linear condensation to the equations does not affect the definition of $\alpha_{\rm cr}$, $S_{\rm cr}$ and $A_{\rho\sigma}$. By a linear condensation is meant the following; suppose from the complete set of atomic levels with populations $N_i : i = 1, \ldots$ a subset of these levels with populations $\mathcal{N}_k : k = 1, \ldots$ is chosen, then putting

$$N_i = \omega_{ik}\mathcal{N}_k \tag{22}$$

and substituting in equations (11) yields a condensed scheme of equations for the $\mathcal{N}_k$. $\alpha_{\rm cr}$ $S_{\rm cr}$, and $A_{\rho\sigma}$ obtained from this condensed set of equations as in (13), (14) and (21) are identical in form with those obtained from the full set of equations. This result is true provided the metastable levels of the full and condensed schemes are the same and in (22), if $i > m$, then k ranges only over values $> m$.

3.2 *Mechanistic viewpoint of recombination*

A number of authors have viewed recombination in a mechanistic or probabilistic way where an electron recombines to some level and the probability that it will diffuse to the ground level is evaluated. This has been used by Seaton (1959) in the low density limit, by D'Angelo (1961, 1965) and by Hinnov & Hirschberg (1962) in the high density limit. In this approach the effective recombination and ionization coefficients are immediately apparent since the electrons are tracked from the continuum to the ground level and vice versa. It is of interest to unify this approach to defining an effective rate for recombination with the approach given in Section 3.1.

Considering the excited states of the atom from the point of view of the jumping bound electron; for an electron on level n, suppose that $p_{n-1}{}^n, \ldots, p_1{}^n$ are the probabilities of moving directly to the level $n-1, \ldots, 1$ in some time interval, and $q_{n+1}{}^n, \ldots, q_\infty{}^n$ the probabilities of the electron moving to the levels $n+1, \ldots, \infty$ (∞ including the continuum). If the lifetime of an atom in an excited state is zero, the probabilities are independent of the time interval and

$$\sum_{i<n} p_i{}^n + \sum_{i>n} q_i{}^n = 1.$$

In practice the q's will be terminated at some sufficiently large n_m, excitation to n_m including excitation to levels $n > n_m$ and ionization. When an electron reaches the ground level it has recombined and is then removed from the group of diffusing electrons. Hence the Markov or probability matrix of the downward diffusion process is

$$D = \begin{bmatrix} 1 & p_1{}^2 & p_1{}^3 & & 0 \\ & 0 & p_2{}^3 & \ldots & \\ 0 & q_3{}^2 & 0 & & 0 \\ & \vdots & & & \\ 0 & & & & 1 \end{bmatrix}. \tag{23}$$

If the recombination rates directly to the levels j are written as r_j, then the number of electrons reaching the ground after one time step is $D_{1j}r_j$ and after one or two time steps is $(D^2)_{1j}r_j$. The collisional radiative recombination coefficient in the mechanistic viewpoint is therefore $(D^\infty)_{1j}r_j$. The elements of the Markov matrix may be obtained in an obvious way from the matrix C. Each column of C must be normalized to unit probability by dividing each element by the diagonal element of C in that column. If $[d_{ii}\delta_{ij}]$ is the normalization matrix then

$$D = \begin{bmatrix} 1 & \bar{C}_{1j}\, d_{jj} & 0 \\ 0 & \bar{C}_{ij}\, d_{jj} - \delta_{ij} & 0 \\ 0 & \bar{C}_{nmj}\, d_{jj} & 1 \end{bmatrix}. \tag{24}$$

The first row elements of D^∞ become

$$\bar{C}_{1j}\, d_{jj}[\delta_{jk} + (\bar{C}_{jk}\, d_{kk} - \delta_{jk}) + \ldots] = \bar{C}_{1j}\, d_{jj}[-\bar{C}_{jk}\, d_{kk}]^{-1}$$

therefore

$$(D^\infty)_{1k} = -\bar{C}_{1j}\bar{C}_{jk}{}^{-1}\ (k \neq 1); \quad (D^\infty)_{11} = 1. \tag{25}$$

Hence the collisional radiative recombination coefficient becomes

$$r_1 - \bar{C}_{1j}\bar{C}_{jk}^{-1}r_k$$

in agreement with the definition in expression (13). The collisional radiative ionization coefficient can be obtained in completely analogous fashion by setting up the Markov matrix for outward diffusion from the ground level, which is

$$U = \begin{bmatrix} 1 & 0 & 0 \\ d_{ii}\bar{C}_{i1} & d_{ii}\bar{C}_{ij} - \delta_{ij} & d_{ii}\bar{C}_{inm} \\ 0 & 0 & 1 \end{bmatrix}. \tag{26}$$

The first column of U^∞ becomes

$$(U^\infty)_{i1} = -\bar{C}_{ij}^{-1}\bar{C}_{j1} \quad (i \neq 1); \qquad (U^\infty)_{11} = 1. \tag{27}$$

Premultiplying by the row matrix $[C_{11}\bar{C}_{1j}]/N_e$ yields the collisional radiative ionization coefficient

$$(C_{11} - \bar{C}_{1i}\bar{C}_{ij}^{-1}\bar{C}_{j1})/N_e.$$

The second term in this expression corrects the total rate of loss from the ground level by subtracting those electrons which return to the ground level without passing through the continuum.

3.3 *Relaxation time scales*

Provided the equilibrium abundances of the excited levels are much lower than that of the ions it is to be expected that these levels will reach an equilibrium rapidly relative to the ion and ground level abundances, and much more rapidly than the ground level reaches its equilibrium in many cases. The actual relaxation times of the excited levels can also be obtained. With N_e and N_+ regarded as uncoupled from the levels, it is apparent that equations (9) constitute a set of linear first-order differential equations. The eigenvalues of the matrix C, that is the solutions λ of

$$|C_{ij} - \lambda\delta_{ij}| = 0 \tag{28}$$

are the exponents of the exponential growth factors $e^{-\lambda t}$ of the levels. The eigenvalue λ_1 corresponding to the ground level will in general be much smaller than the other eigenvalues, and λ_1/N_e is just the collisional radiative ionization coefficient, slight differences being due to the correction for the finite relaxation times of the excited levels. The relaxation of excited levels will be of importance if there is masing among the high levels sustained by inverted populations.

4. ATOMIC PROCESSES

In the expressions for radiative rates given in this section, hydrogenic formulae are used throughout. This is exact in the present work since it is concerned with hydrogen and hydrogenic ions alone. It is also a good approximation for other ions since the l-states are statistically populated to high accuracy, and attention is directed at fairly excited levels in general. For non-hydrogenic ions quantum defect corrections are made to the principal quantum numbers of the lowest levels to ensure that the ionization energies are correct.

The collisional excitation and de-excitation cross-sections presented apply to any ion. Oscillator strengths required for these cross-sections are taken to be hydrogenic in the present calculations, consistent with the radiative expressions. Most of the radiative results are fairly standard; however, to aid high-speed computation simple but accurate approximate formulae have been developed. These are presented as Appendices. The particulars of some of the collision cross-sections have not been published in detail before and so a full development is given as a further Appendix.

4.1 *Bound–bound radiative processes*

The spontaneous emission rate coefficient for hydrogenic ions is

$$A_{n\to n'} = \left(\frac{16\alpha^4 c}{3\sqrt{3}\pi a_0}\right)\frac{z^4 g_{nn'}^{\mathrm{I}}}{n^3 n'(n^2-n'^2)} \quad n'<n. \tag{29}$$

$g_{nn'}^{\mathrm{I}}$ is the bound–bound Kramers–Gaunt factor; n, n' are the principal quantum numbers of the levels, z is the nuclear charge and other notation is conventional. The Einstein B coefficients are given by

$$B_{n\to n'} = A_{n\to n'}\Big/\frac{8\pi h\nu^3}{c^3} \tag{30}$$

$$B_{n'\to n} = \frac{n^2}{n'^2}B_{n\to n'} \tag{31}$$

where $\nu = (z^2 I_{\mathrm{H}}/h)(1/n'^2 - 1/n^2)$ is the frequency of the $n\to n'$ photon. With a Planck radiation field of energy density $u(\nu)$ at temperature T_{r} and dilution W, the photoexcitation rate coefficient is given by

$$u(\nu)\,B_{n'\to n} = \left(\frac{16\alpha^4 c}{3\sqrt{3}\pi a_0}\right)\frac{Wz^4 g_{nn'}^{\mathrm{I}}}{nn'^3(n^2-n'^2)}\Big/[\exp(h\nu/kT_{\mathrm{r}})-1]. \tag{32}$$

The stimulated emission rate coefficient is

$$u(\nu)\,B_{n\to n'} = \left(\frac{16\alpha^4 c}{3\sqrt{3}\pi a_0}\right)\frac{Wz^4 g_{nn'}^{\mathrm{I}}}{n^3 n'(n^2-n'^2)}\Big/[\exp(h\nu/kT_{\mathrm{r}})-1]. \tag{33}$$

A simple expression for $g_{nn'}^{\mathrm{I}}$ is obtained in Appendix A.

4.2 *Bound–free radiative processes*

Analytically continuing the bound–bound formulae into the continuum, the corresponding bound–free rates are obtained. The photoionization rate coefficient from the level n is

$$\int u(\nu)\,B_{n\to\kappa}\,d\kappa = \left(\frac{8\alpha^4 c}{3\sqrt{3}\pi a_0}\right)\frac{Wz^4}{n^5}\int_{I_n/kT_{\mathrm{r}}}^{\infty}\frac{g^{\mathrm{II}}\,dx}{x(e^x-1)}. \tag{34}$$

The stimulated recombination rate coefficient is

$$\int u(\nu)\,B_{\kappa\to n}\,d\kappa = 8\left(\frac{\pi a_0^2 I_{\mathrm{H}}}{kT_{\mathrm{e}}}\right)^{3/2}\left(\frac{8\alpha^4 c}{3\sqrt{3}\pi a_0}\right)\frac{Wz^4}{n^3} \times\exp(I_n/kT_{\mathrm{e}})\int_{I_n/kT_{\mathrm{r}}}^{\infty}\frac{g^{\mathrm{II}}\exp(-T_{\mathrm{r}}x/T_{\mathrm{e}})\,dx}{x[\exp(x)-1]} \tag{35}$$

and the radiative recombination rate coefficient is given by detailed balance as

$$\alpha_n{}^r = 8\left(\frac{\pi a_0{}^2 I_{\rm H}}{kT_{\rm e}}\right)^{3/2}\left(\frac{8\alpha^4 c}{3\sqrt{3}\pi a_0}\right)\frac{z^4}{n^3}\exp\left(I_n/kT_{\rm e}\right)\int_{I_n/kT_{\rm e}}^{\infty}\frac{g^{\rm II}\exp\left(-x\right)dx}{x} \qquad (36)$$

where $I_n = z^2 I_{\rm H}/n^2$, $T_{\rm e}$ is the maxwellian free electron temperature and $g_{i\kappa,n}{}^{\rm II}$ is the analytic continuation of $g_{n'n}{}^{\rm I}$ into the region where $n' = i\kappa$ and κ is real and positive. A simple expression for $g_{i\kappa,n}{}^{\rm II}$ of high accuracy is obtained in Appendix B. The integrals in (34), (35) and (36) are readily evaluated by appropriate gaussian quadratures, although some care is required when the lower integration limit approaches zero.

4.3 *Bound–bound collisional processes*

For the most part in this work, the energies of the colliding particles are much greater than the energy differences of the levels of the atomic transition produced. Further, the dipole matrix element is not zero between such averaged principal quantum levels, so distant encounters are most important, and short range interactions may be neglected. Consequently the Bethe approximation is appropriate for the cross-sections of interest here except perhaps for transitions involving low levels for which the region near to threshold is of greater importance.

Two different expressions, both essentially Bethe approximations are used for collision cross-sections in the present calculations. For transitions due to electron collisions, except for those between closely neighbouring levels, the expressions of Van Regemorter (1962) are used. For electron and proton collisions causing transitions between closely neighbouring levels, strong coupling can occur and so it is preferable to use a better formula in which allowance can be made for this effect. Thus the semi-classical impact parameter (IP) approach is used in this latter case.

4.3.1 *Van Regemorter's cross-sections.* In the Bethe approximation, the cross-section for the excitation by electron collision of the transition $n \to n'$ is

$$Q_{n\to n'} = \frac{8\pi}{\sqrt{3}}\left(\frac{I_{\rm H}}{W_n}\right)\left(\frac{I_{\rm H}}{\Delta E_{nn'}}\right) f_{n\to n'} g \pi a_0{}^2. \qquad (37)$$

W_n is the initial energy of the incident electron, $\Delta E_{nn'}$ the energy difference of the levels n, n' of the transition and $f_{n\to n'}$ is the oscillator strength. g is the Gaunt factor. Van Regemorter (1962) introduces an effective Gaunt factor $\bar{g}$ into (37) which has correct high energy behaviour (Burgess & Tully 1976, to be published) but which is chosen to fit observed results and detailed calculations at lower energies and near threshold. The threshold behaviour of the cross-sections is different for neutral atom and positive ion targets and so $\bar{g}$ is tabulated separately for these two cases. Van Regemorter's formula can therefore be used even for transitions involving low levels, to moderate accuracy, and is used for all transitions here other than those between closely neighbouring levels. The collisional excitation and de-excitation rate coefficients are obtained by integrating over a maxwellian electron distribution. The de-excitation rate for hydrogenic ions is

$$q_{n'\to n}{}^{\rm e} = \frac{2^8}{3}\left(\frac{2\sqrt{\pi}\alpha c a_0{}^2}{3}\right)\frac{n'^3 n^5}{(n'^2-n^2)^4}\frac{g_{nn'}{}^{\rm I}}{z^2}\left(\frac{I_{\rm H}}{kT_{\rm e}}\right)^{1/2} P\left(\frac{\Delta E_{nn'}}{kT_{\rm e}}\right) \quad n'>n \qquad (38)$$

and the excitation rate is

$$q_{n\to n'}{}^{e} = \frac{2^8}{3}\left(\frac{2\sqrt{\pi}\alpha a_0{}^2}{3}\right)\frac{n'^5 n^3}{(n'^2-n^2)^4}\frac{g_{nn'}{}^{I}}{z^2}\left(\frac{I_H}{kT_e}\right)^{1/2}\exp\left(-\Delta E_{nn'}/kT_e\right)P\left(\frac{\Delta E_{nn'}}{kT_e}\right). \tag{39}$$

Van Regemorter also tabulates the function P for neutral atom and positive ion targets.

4.3.2 *Impact parameter cross-sections.* The cross-section for the $n\to n'$ transition may be resolved in terms of the contributions from different angular momenta of the colliding particle. In the semi-classical case this gives

$$Q_{n\to n'} = \int_0^\infty P_{n\to n'}(R_i)\,2\pi R_i\,dR_i$$

where with impact parameter R_i and initial state n, $P_{n\to n'}$ is the probability of the $n\to n'$ transition occurring. Now the Born approximation is too large at low energies where the contribution from small impact parameters is overestimated. Here the primary concern is with optically allowed transitions for which a large contribution comes from distant encounters. Thus an improvement is to be expected if a cut-off is introduced at small impact parameters, say at R_0 where R_0 is comparable with atomic dimensions (Seaton 1955). For $R_i > R_0$ this should be satisfactory provided conservation of probability is satisfied; that is provided $P_{n\to n'}(R_i)\leq 1$. When the coupling is strong it is expected that, for $R_i < R_1$ where $P_{n\to n'}(R_1) = \frac{1}{2}$, the function $P_{n\to n'}$ will be oscillatory with mean value $\frac{1}{2}$, assuming a two-level atom. Thus in weak coupling where $P_{n\to n'}(R_i)\leq\frac{1}{2}$ for all R_i, Seaton takes

$$Q_{n\to n'}{}^{\omega} = \int_{R_0}^\infty P_{n\to n'}(R_i)\,2\pi R_i\,dR_i, \tag{40}$$

and for strong coupling, Seaton suggests

$$Q_{n\to n'}{}^{S} = \tfrac{1}{2}\pi R_1{}^2 + \int_{R_1}^\infty P_{n\to n'}(R_i)\,2\pi R_i\,dR_i. \tag{41}$$

Simple properly symmetrized expressions for $P_{n\to n'}(R_i)$ can be obtained in the semi-classical impact parameter method (Alder *et al.* 1956). These have been derived for neutral targets by Seaton (1962). Cross-sections are also required here for positive ion targets and these have been derived by Burgess (1964b). A full development is in Appendix C. The formulae are summarized in this section. Let k_n and $k_{n'}$ be the initial and final wave numbers of the colliding particle. For electrons: putting $\xi = (z/a_0)\left|1/k_n - 1/k_{n'}\right|$ and $\delta = R^c\left|k_n - k_{n'}\right|$, the strong coupling condition is given by the solution $\delta_1 (= R_1{}^c\left|k_n - k_{n'}\right|)$ of

$$8\left(\frac{I_H}{\Delta E_{nn'}}f_{n\to n'}\right)\frac{k_n k_{n'}}{(k_n k_{n'} R_1{}^c + z/a_0)^2}X(\xi,\delta_1) = 1. \tag{42}$$

R^c is the distance of closest approach. Thus in weak coupling

$$Q_{n\to n'}{}^{W} = \frac{I_H}{W_n}\left[8\left(\frac{I_H}{\Delta E_{nn'}}f_{n\to n'}\right)Y(\xi,\delta_0)\right]\pi a_0{}^2 \tag{43}$$

and in strong coupling

$$Q_{n\to n'}{}^{\mathrm{s}} = \frac{I_{\mathrm{H}}}{W_n}\left[8\left(\frac{I_{\mathrm{H}}}{\Delta E_{nn'}}f_{n\to n'}\right)Y(\xi,\delta_1)+\frac{z}{a_0}R_1{}^{\mathrm{c}}+\tfrac{1}{2}k_nk_{n'}(R_1{}^{\mathrm{c}})^2\right]\pi a_0{}^2 \quad (44)$$

where $\delta_0 = R_0{}^{\mathrm{c}}|k_n-k_{n'}|$ and $R_0{}^{\mathrm{c}}$ is the smaller of the mean atomic radii in states n and n'.

For protons: putting $\xi = (z/a_0)(m/m_{\mathrm{e}})|1/k_{n'}-1/k_n|$ and $\delta = R^{\mathrm{c}}|k_n-k_{n'}|$, the strong coupling condition is given by the solution δ_1 of

$$8\left(\frac{I_{\mathrm{H}}}{\Delta E_{nn'}}f_{n\to n'}\right)\frac{k_nk_{n'}}{(m_{\mathrm{e}}/m)^2[k_nk_{n'}R_1{}^{\mathrm{c}}-(m/m_{\mathrm{e}})(z/a_0)]^2}X(-\xi,\delta_1) = 1. \quad (45)$$

Thus in weak coupling

$$Q_{n\to n'}{}^{\mathrm{w}} = \frac{I_{\mathrm{H}}}{W_n}\left[8\left(\frac{I_{\mathrm{H}}}{\Delta E_{nn'}}f_{n\to n'}\right)Y(-\xi,\delta_0)\right]\left(\frac{m}{m_{\mathrm{e}}}\right)\pi a_0{}^2 \quad (46)$$

and in strong coupling

$$Q_{n\to n'}{}^{\mathrm{s}} = \frac{I_{\mathrm{H}}}{W_n}\left[8\left(\frac{I_{\mathrm{H}}}{\Delta E_{nn'}}f_{n\to n'}\right)Y(-\xi,\delta_1)+\left(\frac{m_{\mathrm{e}}}{m}\right)^2 \times\left\{\tfrac{1}{2}k_nk_{n'}(R_1{}^{\mathrm{c}})^2-\frac{m}{m_{\mathrm{e}}}\frac{z}{a_0}R_1{}^{\mathrm{c}}\right\}\right]\left(\frac{m}{m_{\mathrm{e}}}\right)\pi a_0{}^2. \quad (47)$$

δ_0 is as before, m is the reduced mass of the proton and m_{e} is the electron mass. The analytic expressions for the functions X and Y are given in Appendix C together with a numerical tabulation. The formulae for X and Y apply for $W_> \geq 1{\cdot}25\ \Delta E_{nn'}$ (where $W_>$ is the greater of W_n and $W_{n'}$), the region closer to threshold being deduced from the appropriate threshold laws (*cf.* Appendix C). These cross-sections have been found to give very satisfactory results for optically allowed transitions.

Some further comment is required on these cross-sections. In establishing the condition for strong coupling, it was assumed that the atom had only two levels. For collisions with highly-excited states there are many nearby levels. Consequently in the strong coupling region the assumption that the mean value of $P_{n\to n'}$ is $\frac{1}{2}$ is unrealistic since an electron can escape from the upper level to levels other than the initial level in the course of the collision. The true mean value will be less than $\frac{1}{2}$. Further, since the proton collisions occur more slowly than the electron collisions, the mean $P_{n\to n'}$ in the strong coupling region for proton collisions will probably be less than for electrons. The complete quantum mechanical solution of collisions with highly-excited states required to clarify these points is a matter of considerable difficulty. However, some assessment of the reliability of the present cross-section expressions for collisions with highly-excited states can be made by comparison with the work of Percival & Richards (1970, 1971a, 1971b) who have developed a Correspondence Principle approach to the problem. For transitions between states with initial and final principal quantum numbers n and n', their basic results apply for $2/n < W_n/I_{\mathrm{H}} < 2$ with n large and $s(=|n-n'|)$ small. W_n is the incident particle energy. Their results for electron collisions with hydrogen atoms have been extended to higher energies by Richards (1973), and to lower energies, in the range $4/n^2 < W_n/I_{\mathrm{H}} < 2/n$ by Banks, Percival & Richards (1973). A comparative tabulation of Impact Parameter (IP), Van Regemorter (VR) and Correspondence Principle (PR) cross-sections for collisions of electrons with hydrogen atoms is shown in Table I.* The tabulations are for incident energies

* We use the notation $1{\cdot}23^4$ for $1{\cdot}23\times10^4$.

TABLE I

Comparison of Impact parameter, Percival & Richards (1970), *and Van Regemorter* (1962) *cross-sections for e–H collisions between levels n and n′ where* $s = n' - n$. *For* $W_n/I_H = 0{\cdot}0063$; $n = 10, 30, 100$ *and* $W_n/I_H = 0{\cdot}063$; $n = 10, 30$ *the results of Banks* et al. (1973) *are given.*

		$W_n/I_H = 0{\cdot}0063$			$W_n/I_H = 0{\cdot}063$			$W_n/I_H = 0{\cdot}63$		
n	s	Q_{PR}	Q_{IP}	Q_{VR}	Q_{PR}	Q_{IP}	Q_{VR}	Q_{PR}	Q_{IP}	Q_{VR}
	1	1.19^{4}	2.85^{4}	8.50^{5}	3.55^{4}	7.17^{4}	2.88^{5}	4.01^{4}	3.74^{4}	4.63^{4}
	2	4.40^{3}	3.22^{3}	5.08^{4}	9.69^{3}	1.02^{4}	2.21^{4}	5.25^{3}	2.66^{3}	3.68^{3}
10	3	2.36^{3}	9.03^{1}	1.05^{4}	4.34^{3}	1.68^{3}	4.67^{3}	1.79^{3}	5.71^{2}	8.85^{2}
	4	1.48^{3}	3.94^{0}	3.60^{3}	2.42^{2}	4.61^{2}	1.65^{3}	8.69^{2}	1.97^{2}	3.33^{2}
	6	7.34^{2}	9.51^{-2}	8.54^{2}	1.04^{3}	7.63^{1}	4.07^{2}	3.29^{2}	4.64^{1}	8.91^{1}
	10				3.46^{2}	8.76^{0}	7.78^{1}	1.03^{2}	8.24^{0}	1.84^{1}
	1	5.67^{6}	1.26^{7}	2.48^{8}	7.61^{6}	1.40^{7}	3.70^{7}	3.80^{6}	3.82^{6}	4.92^{6}
	2	1.88^{6}	2.06^{6}	1.62^{7}	1.49^{6}	1.41^{6}	2.54^{6}	3.77^{5}	2.37^{5}	3.47^{5}
30	3	9.38^{5}	5.04^{5}	3.40^{6}	5.52^{5}	2.47^{5}	5.38^{5}	1.07^{5}	4.62^{4}	7.44^{4}
	4	5.60^{5}	9.28^{4}	1.15^{6}	2.70^{5}	7.03^{4}	1.81^{5}	4.56^{4}	1.47^{4}	2.54^{4}
	6	2.62^{5}	6.84^{3}	2.34^{5}	9.89^{4}	1.17^{4}	4.05^{4}	1.46^{4}	2.99^{3}	5.77^{3}
	10	9.61^{4}	1.80^{2}	3.29^{4}	2.84^{4}	1.19^{3}	6.65^{3}	3.81^{3}	4.25^{2}	9.67^{2}
	1	3.39^{9}	6.33^{9}	5.11^{10}	2.97^{9}	3.13^{9}	6.53^{9}	5.85^{8}	5.91^{8}	7.95^{8}
	2	8.45^{8}	8.18^{8}	3.33^{9}	3.12^{8}	2.59^{8}	4.35^{8}	5.06^{7}	3.60^{7}	5.36^{7}
100	3	3.47^{8}	2.32^{8}	6.67^{8}	9.01^{7}	4.68^{7}	8.81^{7}	1.28^{7}	6.88^{6}	1.09^{7}
	4	1.78^{8}	6.39^{7}	2.13^{8}	3.83^{7}	1.39^{7}	2.84^{7}	4.97^{6}	2.12^{6}	3.55^{6}
	6	6.75^{7}	8.63^{6}	4.31^{7}	1.18^{7}	2.45^{6}	5.82^{6}	1.39^{6}	4.02^{5}	7.34^{5}
	10	1.91^{7}	5.53^{5}	5.90^{6}	2.76^{6}	2.67^{5}	8.13^{5}	3.02^{5}	4.98^{4}	1.04^{5}

equivalent to temperatures 10^3, 10^4 and 10^5 K ($W_n = kT_e$). Generally $Q_{IP} \sim Q_{PR}$ for $s \lesssim 3$. Q_{VR} is larger than Q_{IP} in general and $Q_{VR} \sim Q_{PR}$ for $s \sim 4$. For large s, Q_{PR} becomes greater than both Q_{IP} and Q_{VR} because of the greater importance of classical binary encounter contributions contained in Q_{PR}. In the present work Q_{IP} is used for $s \leq 3$ and Q_{VR} for $s > 3$. This is a compromise which gives fairly good agreement with Q_{PR} for the most important neighbouring transitions yet applies well to low levels, hydrogenic ions and non-hydrogenic systems.

There is an additional uncertainty concerning the behaviour of the cross-sections for collisions with neutral hydrogen at threshold. For such collisions, the dipole coupling between degenerate levels will cause the cross-section to be finite at threshold analogous to the positive ion case. All the above cross-sections give a zero threshold for collisions with neutrals. The magnitude of the threshold cross-section is difficult to calculate; however, the effect can be assessed roughly by using the same threshold as for hydrogenic ions. The consequences for hydrogen population structure is considered in Section 7 (*cf.* Table 7).

4.4 *Bound–free collisional processes*

For the ionization cross-section, the ECIP results of Burgess (1964a) (*cf.* also Burgess & Percival 1968), which unite a properly symmetrized classical binary encounter theory for close collisions with an impact parameter treatment for the distant collisions, are used. This formulation therefore has the correct behaviour at high and low energies. The ionization cross-section is

$$Q_{n\to\epsilon} = Q_{n\to\epsilon}{}^{c} + Q_{n\to\epsilon}{}^{IP}. \tag{48}$$

where $Q_{n\to\epsilon}{}^{c}$ is the binary encounter contribution which is taken as

$$Q_{n\to\epsilon}{}^{c} = \frac{\pi e^4}{W_n + I_n}\left[\left(\frac{1}{I_n} - \frac{1}{W_n}\right) - \frac{\ln(W_n/I_n)}{W_n + I_n}\right] \tag{49}$$

in the present work. The impact parameter contribution is obtained by extending the formula of Section 4.3.2 into the continuum and integrating over permissible ejected electron energies. It is convenient to write

$$Q_{n\to\epsilon}{}^{IP} = \left(\frac{I_H}{W_n}\right)\left(\frac{I_H}{I_n}\right) I^{IP}(W_n)\,\pi a_0{}^2. \tag{50}$$

The cut-off radius in $I^{IP}(W_n)$ must be determined. Burgess takes $R_0{}^{c} = \bar{r} + \bar{d}$ for weak coupling where $\bar{r}$ is the mean atomic radius and

$$\bar{d} = \frac{2I_H\sqrt{(W_n + I_n - \epsilon)/\epsilon}}{W_n + I_n}$$

and the usual expression for $R_1{}^{c}$ in the case of strong coupling. The collisional ionization rate coefficient is finally obtained as

$$q_{n\to\epsilon} = (8\sqrt{\pi}\alpha c a_0{}^2)\left(\frac{I_H}{kT_e}\right)^{1/2}\frac{n^2}{z^2}\exp(-I_n/kT_e)\int_0^\infty G\exp(-\zeta)\,d\zeta \tag{51}$$

and the three-body recombination rate coefficient is

$$\alpha_n{}^3 = 2^6\pi^2(\alpha c a_0{}^5)\left(\frac{I_H}{kT_e}\right)^2\frac{n^4}{z^2}\int_0^\infty G\exp(-\zeta)\,d\zeta. \tag{52}$$

$$\zeta = \frac{(W_n - I_n)}{kT_e}$$

and

$$G = \left[\left(\frac{W_n/I_n - 1}{W_n/I_n + 1}\right) - \frac{W_n/I_n}{(W_n/I_n+1)^2}\ln\left(\frac{W_n}{I_n}\right) + \tfrac{1}{4}I^{IP}(W_n)\right].$$

4.5 *The statistical balance equations*

Equations (8) can be reconstituted using the formulae for reaction rates developed in the previous sections. It is usual to write the equations in terms of the deviations of the populations from those which would prevail in thermodynamic equilibrium. The deviation b_n is defined by

$$N_n = N_e N_+ 8\left(\frac{\pi a_0{}^2 I_H}{kT_e}\right)^{3/2} n^2\exp(I_n/kT_e)\,b_n. \tag{53}$$

Then equations (8) in equilibrium give, on appropriate reorganization and cancellation,

$$\begin{aligned}
&\sum_{n'>n}\frac{g_{nn'}{}^I\exp(I_{n'}/kT_e)}{nn'(n'^2-n^2)}b_{n'} + \sum_{n'\neq n}\frac{Wg_{nn'}{}^I\exp(I_{n'}/kT_e)}{[\exp(h\nu/kT_r)-1]\,n'n|n^2-n'^2|}b_{n'} \\
&\qquad + \sum_{n'\neq n}\frac{\rho}{t_e{}^{1/2}}\frac{n'^5n^5g_{nn'}{}^I}{(n^2-n'^2)^4}P\left(\frac{\Delta E_{nn'}}{kT_e}\right)\exp(I_>/kT_e)\,b_{n'} \\
&\qquad + \frac{1}{2n^3}\exp(I_n/kT_e)\left[\int_{I_n/kT_e}^\infty\frac{g^{II}\exp(-x)}{x}\,dx\right. \\
&\qquad\qquad \left. + W\int_{I_n/kT_r}^\infty\frac{g^{II}\exp(-T_rx/T_e)}{x[\exp(x)-1]}\,dx\right] \\
&= \left\{\sum_{n''<n}\frac{g_{nn''}{}^I}{nn''(n^2-n''^2)} + \sum_{n'\neq n}\frac{Wg_{nn'}{}^I}{[\exp(h\nu/kT_r)-1]}\frac{1}{nn'|n^2-n'^2|}\right\}\exp(I_n/kT_e)\,b_n \\
&\qquad + \sum_{n'\neq n}\frac{\rho}{t_e{}^{1/2}}\frac{n'^5n^5g_{nn'}{}^I}{(n'^2-n^2)^4}P\left(\frac{\Delta E_{nn'}}{kT_e}\right)\exp(I_>/kT_e)\,b_n \\
&\qquad + \frac{1}{2}\frac{W}{n^3}\exp(I_n/kT_e)\int_{I_n/kT_r}^\infty\frac{g^{II}\,dx}{x[\exp(x)-1]}\,b_n \\
&\qquad + \frac{3^2}{2^6}\frac{\rho}{t_e{}^{1/2}}\int_0^\infty G\exp(-\zeta)\,d\zeta(b_n-1)
\end{aligned} \tag{54}$$

where scaled temperatures and electron density (*cf.* BKMcW) are

$$t_e = \left(\frac{kT_e}{I_H}\right)\frac{1}{z^2}\qquad t_r = \left(\frac{kT_r}{I_H}\right)\frac{1}{z^2}\qquad \rho = 2^5\sqrt{\frac{\pi}{3}}\frac{\pi a_0{}^3 N_e}{\alpha^3 z^7}. \tag{55}$$

$I_>$ denotes the greater of I_n and $I_{n'}$ and $P(\Delta E_{nn'}/kT_e)$ is used to describe both the Van Regemorter and impact parameter collisional rates and also incorporates the effect of proton collisions.

5. NUMERICAL SOLUTION

The set of equations (54) presents a considerable computational problem. This arises from the fact that interest is currently directed at very highly-excited states. When dielectronic recombination is included (Burgess & Summers 1969) it proves necessary to include up to 1000 levels. Contrast this with the treatment of BKMcW where primarily the recombination of hydrogen and hydrogenic ions was of interest, for which 20 levels proved sufficient. Clearly a complete set of 1000 levels is outside the storage capacity of current computers and some technique is required to render the problem tractable.

A differential equation approach has been developed by Seaton (1964) and elaborated by other authors, while Sejnowski & Hjellming (1969) have used an iterative procedure. These methods tend to have some limitations which will be considered later. The method adopted here is one based on Lagrangian interpolation (Burgess & Summers 1969) which has proved extremely satisfactory and stable. Apart from the first one or two levels the populations or alternatively the b_n's vary smoothly with change in the principal quantum number n. This suggests that a representative set of levels may be selected from the complete set of levels. The population of each level is then represented by a Lagrangian interpolation over the representative levels. Thus the complete set of equations can be rewritten in terms of a considerably reduced number of representative equations. As mentioned in Section 3.1 this linear condensation (equation (22)) does not affect the definition of the collisional radiative coefficients while the condensed matrix is readily inverted to yield the equilibrium populations of the representative levels.

The interpolating variable may be chosen arbitrarily. A suitable variable is found to be $1/(n+10)^2$ where n is the principal quantum number. The order of interpolation is again a matter of choice but it is preferable to use an odd-point formula since this gives continuity of both interpolated populations and their gradients through the representative levels. Representative levels may be freely chosen provided care is exercised in selecting sufficient low levels. The asymptotic limit $b_n \to 1$ as $n \to \infty$ is used as a node of the interpolation scheme at the top of the representative level set, while some allowance is made for including only a finite number of levels by lowering the continuum to the energy of the uppermost level of the complete set. More elaborate extrapolations are found to be unnecessary due to the ease of including sufficient levels for all purposes. The b_n's of the more highly-excited states are all near unity, so greater sensitivity is obtained by arranging the program to solve for the c_n's ($c_n = b_n - 1$). At very low electron temperatures, difficulties arise since the c_n's of the lowest levels tend to -1 (in the presence of a radiation field) while the exponential factors in the populations (*cf.* equation (53)) become very large. For these levels $\exp(I_n/kT_e)\, b_n$ remains finite. To eliminate the computational divergences, it is necessary to recast equations (54) for the lowest levels in terms of $\exp(I_n/kT_e)\, b_n$ as the unknowns with the remainder still in terms of the c_n's. This procedure is quite satisfactory provided the transition level between the two forms of equations is not affected by the interpolation scheme. Output information includes α_{cr}, S_{cr}, b_n's, c_n's, the populations N_n and the Δb_n's ($\Delta b_n = b_n - b_{n-1}$).

5.1 *Errors*

The errors in the calculation arise from two sources. First there are the cumulative rounding errors in the machine computations and second the inaccuracy

introduced by the interpolation method. The first source of error was assessed by 'running' the program on machines of different word length from which it is evident that the collisional radiative coefficients have fractional errors $\sim 10^{-6}$, the intermediate level c_n's $\sim 10^{-5}$ and the high level c_n's $\sim 10^{-3}$ for computations on 48-bit word machines. On the second source of error, extensive variation of interpolating variables, total number of levels and number of representative levels indicate a fractional error $\sim 10^{-2}$ can be expected at levels $n \sim 300$ with greater accuracy for lower levels when ~ 30 representative levels are used. These errors are well within the tolerances set by uncertainty in the cross-section data.

6. COLLISIONAL–RADIATIVE RECOMBINATION AND IONIZATION OF HYDROGENIC IONS

The subject is treated in two subsections. In Section 6.1 the probabilistic method is demonstrated at high densities. The intermediate density situation is considered in Section 6.2 in comparison with the work of BKMcW. The definition of the recombination coefficient in the low density limit is not ambiguous and has been described by Seaton (1959), Baker & Menzel (1938) and by Menzel & Baker (1937), consequently this case is not discussed here. The calculations to be described are rather more complete than those of previous workers, while the cross-section data used is probably the more reliable.

6.1 *Hydrogen recombination at high electron density*

At fairly low temperatures $kT_e \lesssim 0{\cdot}1$ eV and at high electron densities, recombination in hydrogen is dominated by the three-body recombination coefficient. It is interesting to consider the collisional radiative recombination coefficient in the limit of high electron density in which radiative processes may be neglected. Proton collisions are also omitted in this section. The variation with temperature of the three-body recombination rate to a given n level does not reveal the true temperature dependence of the full collisional radiative rate since a fairly long series of electron temperature-dependent transitions may have to occur before a recombining electron reaches the ground level. In this situation where many collisional transitions are involved it is easy to treat the process from the probabilistic description. Hinnov & Hirschberg (1962) attempt to locate that n level, say n^*, such that all electrons recombining to levels $n < n^*$ ultimately reach the ground level and those recombining to levels $n \geq n^*$ ultimately reionize without ever reaching the ground level. More precisely, if ${}^nP_1$ is the probability that an electron on level n will ultimately reach the ground level, then n^* is defined by

$$\sum_{n=1}^{n^*} \alpha_n{}^3 = \sum_{n=1}^{\infty} \alpha_n{}^3 {}^nP_1. \tag{56}$$

At sufficiently low temperatures such that the probability of collisional transitions between adjacent levels is much larger than the rate of ionization, they concluded that n^* is approximately defined by

$$\frac{n^{*2}}{(n^*-1)^2} \exp\left[(I_{n^*} - I_{n^*-1})/kT_e\right] = 1. \tag{57}$$

With a Thomson (1912) classical three-body recombination rate of

$$\alpha_n{}^3 = 2{\cdot}305^{-31} \left(\frac{I_H}{kT_e}\right)^2 \frac{1}{z^2} n^4 \tag{58}$$

the collisional radiative recombination coefficient becomes

$$\frac{\alpha_{cr}}{N_e} \simeq 0{\cdot}461^{-31}\left(\frac{I_H}{kT_e}\right)^{9/2}\frac{1}{z^2} \tag{59}$$

in the high density limit. This treatment is valid provided $n^* \gg 1$, which condition requires that $T_e < 2\times 10^4$ K. At higher temperatures low levels begin to have an effect, which disturbs this simple $T_e^{-9/2}$ behaviour of α_{cr}/N_e. The problem may be investigated with the Markov matrix approach of Section 3.2.

A preliminary most simple approximation to the D matrix in the limit $N_e \to \infty$, and at fairly low temperatures, is to include only adjacent transitions. Using Van Regemorter's cross-sections (*cf.* Section 4.3.1) this gives

$$\begin{aligned} p_{n-1}{}^n &= \frac{q_{n\to n-1}}{q_{n\to n-1}+q_{n\to n+1}} \\ &= \frac{P(\Delta E_{n,n-1}/kT_e)}{\exp(-2I_H/n^3kT_e)\,P(\Delta E_{n,n+1}/kT_e)+P(\Delta E_{n,n-1}/kT_e)} \end{aligned} \tag{60}$$

and

$$q_{n+1}{}^n = \frac{P(\Delta E_{n,n+1}/kT_e)}{\exp(2I_H/n^3kT_e)\,P(\Delta E_{n,n-1}/kT_e)+P(\Delta E_{n,n+1}/kT_e)}.$$

Note that $p_{n-1}{}^n + q_{n+1}{}^n = 1$ and all the remaining p's and q's are zero. On powering, the D matrix convergence to D^∞ is rapid. The final collisional radiative recombination coefficient is obtained using the three-body recombination rate expression (58) which is the formula used by BKMcW in their calculations (*cf.* Section 6.2). The results are shown in curve 1 of Fig. 1. As can be seen, at low temperatures the slope of the curve is nearly up to a gradient of 9/2. Only the first 20 levels have been

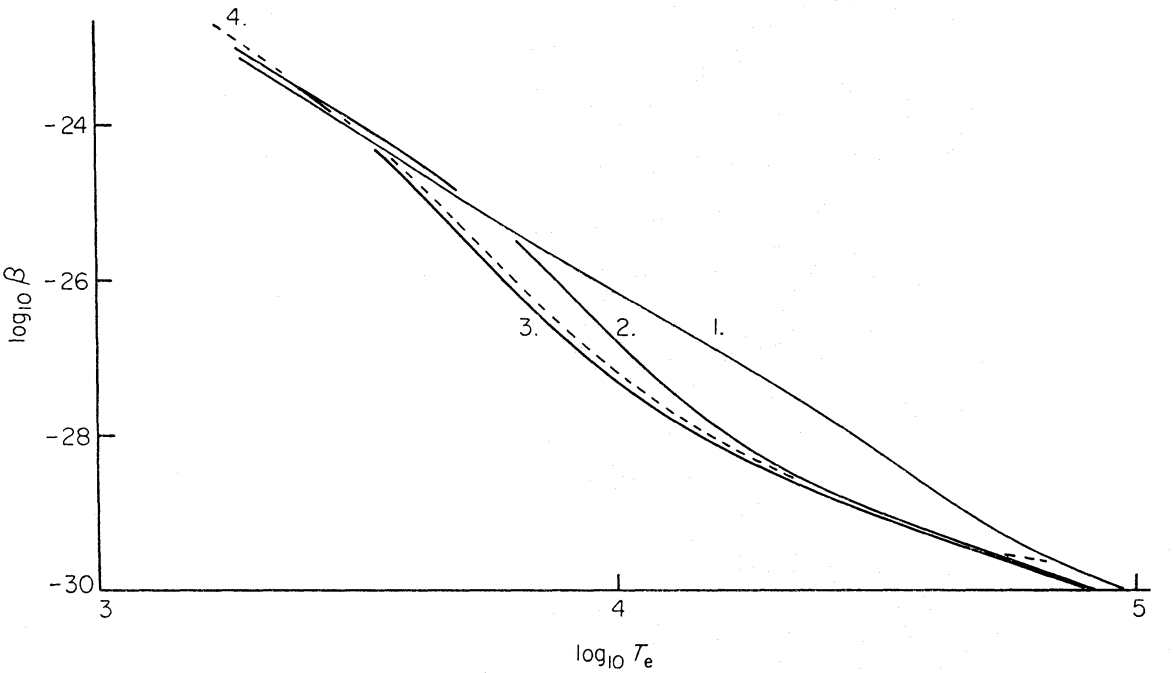

FIG. 1. *$H^+ + e$ collisional radiative recombination. $\beta = lim(\alpha_{cr}/N_e)$ as $N_e \to \infty$. 1, Adjacent collisional transitions only. 2, Adjacent and all collisional transitions from $n = 2$ level. 3, Adjacent and all collisional transitions from $n = 2$ and 3 levels. 4, Results of BKMcW.*

included here. Further levels would be needed to extend to lower temperatures. At higher temperatures the curve is fairly widely different from the accurate curve of BKMcW obtained from statistical balance. Now at the higher temperatures the lowest levels ($n = 2, 3$) are the ones which most critically affect the coefficient. Thus as a better approximation, in curve 2, all the collisional transitions from $n = 2$ have been introduced into the D matrix.

$$p_1{}^2 = \frac{q_{2\to 1}}{q_{2\to 1} + \sum_{j>2} q_{2\to j}} \tag{61}$$

$$q_n{}^2 = \frac{q_{2\to n}}{q_{2\to 1} + \sum_{j>2} q_{2\to j}} \quad n > 2.$$

This produces a considerable improvement particularly at the higher temperatures where $n = 2$ is the dominant level. Improvement in the probabilities from the $n = 3$ level corrects the behaviour at slightly lower temperatures (curve 3 of Fig. 1). Slight differences from the BKMcW curve are due to differences in the bound–bound cross-sections used. BKMcW use Grysinski (1959) classical cross-sections which have incorrect high energy behaviour.

6.2 *Hydrogenic ion recombination at intermediate densities*

The statistical balance methods of this paper are similar to those of BKMcW and consequently detailed comparison with their work is of value, particularly since the cross-section data used here is rather better than that of BKMcW. In view of the temperatures achieved in present plasma experiments it is also advantageous to give a wider temperature range than BKMcW. As has been mentioned, their work was concerned only with recombination and ionization of hydrogen and hydrogenic ions and not with population structure, so it was sufficient for them to consider the first 20 levels with some extrapolation to higher levels. No external radiation field was included in their work and the bound–bound cross-sections were the Grysinski expressions. The ionization rate was the Thomson classical formula.

In Section 4.5 it was convenient to scale the electron density and temperature with nuclear charge in the equations (54). This was discussed by BKMcW in which it was shown that for hydrogenic systems of charge z, α_{cr}/z was obtainable from the $z = 1$ equations in which simply N_e was replaced by N_e/z^7 and T_e by T_e/z^2. These scaling laws therefore enabled all hydrogenic systems to be described simultaneously. The scaling however is not quite exact since the effective Gaunt factors (*cf.* Section 4.3.1) are z-dependent. However, they are nearly constant so the scaling is a good approximation. The scaled collisional radiative recombination and ionization coefficients do not describe hydrogen $z = 1$ so well since the behaviour of the collision cross-sections at threshold is different for neutral and charged species. Consequently results must be given separately for hydrogen and hydrogenic ions.

In the present results a dilution $W = 0$ was assumed. However, at very low temperatures the collisional ionization rate is negligible and a direct ground state to continuum dilution must be introduced to prevent divergences. This does not affect α_{cr}. In these calculations 21 representative levels were taken and a total of 120 levels considered. Impact parameter cross-sections were used for $\Delta n \leq 3$, and

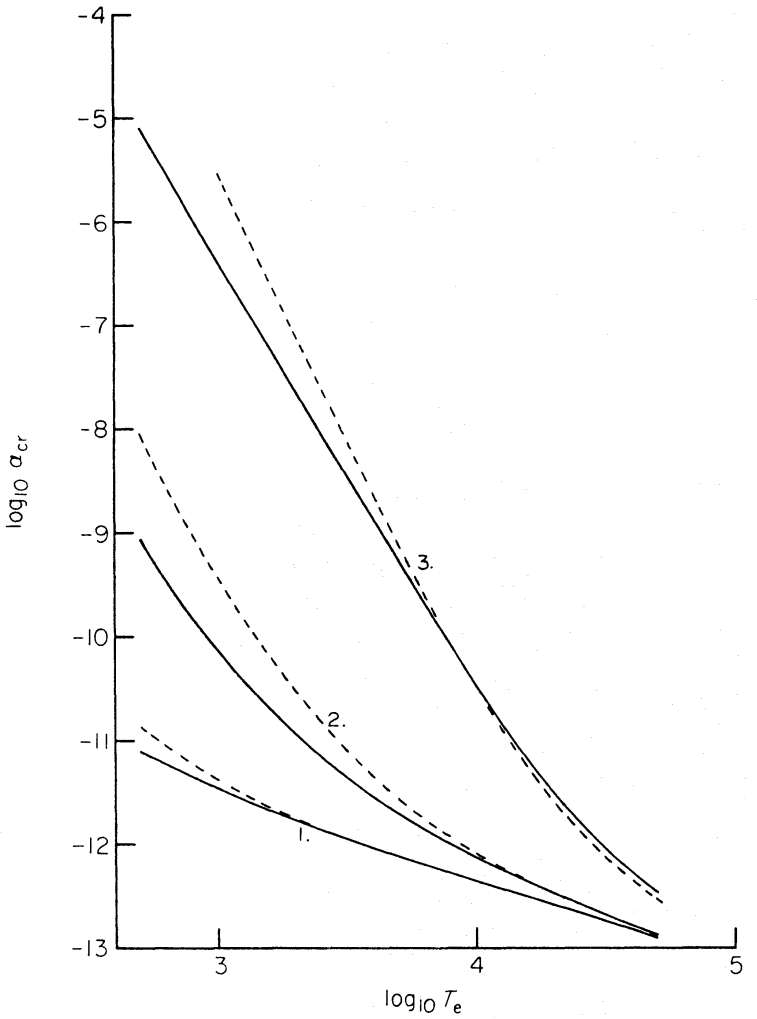

FIG. 2. *$H^+ + e$ collisional radiative recombination.* 1, $N_e = N_p = 10^8\ cm^{-3}$, $T_p = T_e$, $W = 0$. 2, $N_e = N_p = 10^{12}\ cm^{-3}$, $T_p = T_e$, $W = 0$. 3, $N_e = N_p = 10^{16}\ cm^{-3}$, $T_p = T_e$, $W = 0$. *BKMcW results dashed.*

Van Regemorter's cross-sections for $\Delta n > 3$. Proton collisions were included with $T_p = T_e$ and $N_p = N_e$; however, they give only a very small correction to α_{cr} and S_{cr}. Computations were carried out for hydrogen $z = 1$ and for the hydrogenic ion $z = 4$; proton collisions being neglected in the latter case. The results for $z = 4$ are expressed in terms of reduced coefficients, temperatures and densities. In illustration α_{cr} is graphed in Fig. 2 for $z = 1$ and α_{cr}/z in Fig. 3 for $z = 4$, the results of BKMcW also being graphed for comparison.

At the lowest density, recombination is mainly radiative which occurs most strongly to the lowest levels. Collisions are unimportant and so the temperature dependence of α_{cr} is $1/T_e^{1/2}$ which is that of the radiative recombination coefficient. As the electron density increases three-body recombination becomes more active particularly at the lower temperatures where the rate is largest, and α_{cr} increases. At these lower temperatures recombination occurs through more excited levels where collisional processes are strong. This changes the temperature dependence of α_{cr} to $\sim 1/T_e^4$ at the highest density considered, which approaches the form suggested by Hinnov & Hirschberg (1962) for the ∞ density case. At higher temperatures the collisional processes require greater densities before they become

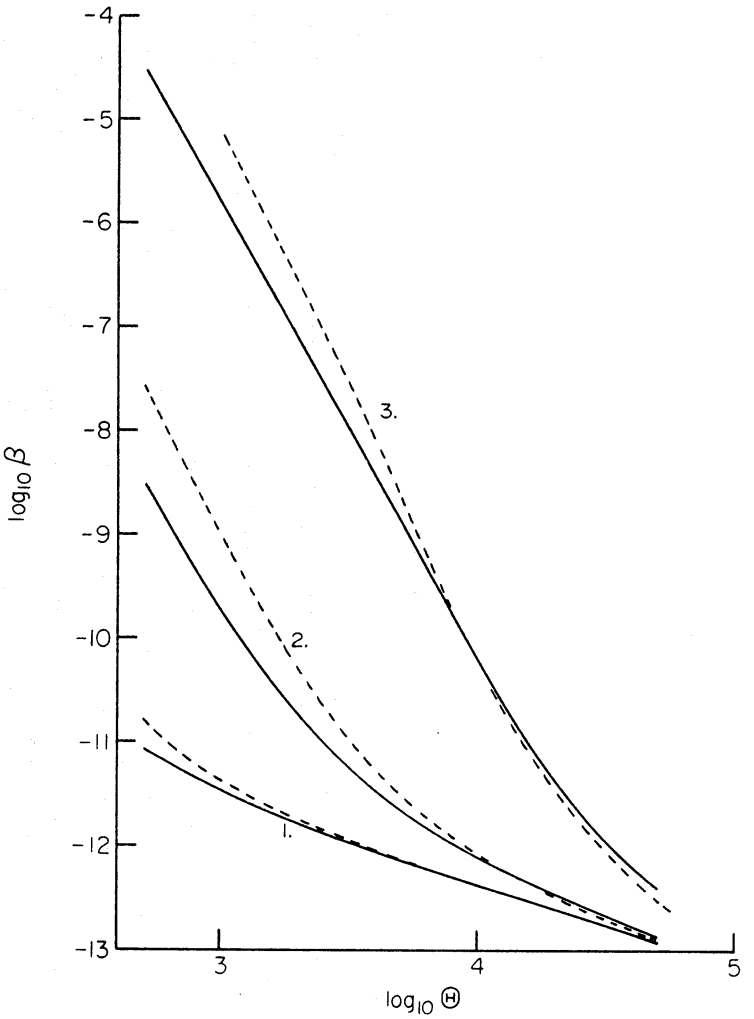

FIG. 3. $X^{+4}+e$ *collisional radiative recombination.* $\beta = \alpha_{cr}/z$, $\rho = N_e/z^7$, $\Theta = T_e/z^2$. 1, $\rho = 10^8\ cm^{-3}$, $N_p = 0$, $W = 0$. 2, $\rho = 10^{12}\ cm^{-3}$, $N_p = 0$, $W = 0$. 3, $\rho = 10^{16}\ cm^{-3}$, $N_p = 0$, $W = 0$. *BKMcW results dashed.*

dominant. Consequently α_{cr} remains closer to the radiative limit at the higher temperatures. As can be seen from the graphs, agreement with BKMcW is good except at lower temperatures and higher densities. The deviations which do occur are principally due to cross-section differences. S_{cr} differs more widely between the present results and those of BKMcW (up to factors ~ 2). This is to be expected since the ground ionization rate is directly involved. The agreement is better in the case of hydrogenic ions for which the cross-section expressions are more similar.

A full tabulation of α_{cr} and S_{cr} is given in Tables II and III for $z = 1$ and in Tables IV and V for $z = 4$.

7. HYDROGEN POPULATION STRUCTURE

Results are given in this section for the population structure of hydrogen using the methods developed in the previous sections. Impact parameter cross-sections are used for $\Delta n \leq 3$ and a total of 500 levels with about 30 representative levels considered. The dilution of the radiation field is constant for all levels unless

TABLE II

Tabulation of α_{cr} $(cm^3\ s^{-1})$ *for hydrogen* $z = 1$. $N_p = N_e$, $T_p = T_e$, $W = 0$

N_e cm^{-3}	1.00^{8}	1.00^{10}	1.00^{12}	1.00^{14}	1.00^{16}	1.00^{18}	1.00^{20}
T_e K							
2.00^{2}	4.05^{-11}	6.74^{-10}	3.70^{-8}	3.64^{-6}	3.64^{-4}	3.64^{-2}	3.64^{0}
5.00^{2}	7.85^{-12}	3.37^{-11}	8.10^{-10}	6.97^{-8}	6.96^{-6}	6.96^{-4}	6.96^{-2}
1.00^{3}	3.29^{-12}	8.03^{-12}	7.47^{-11}	4.08^{-9}	3.98^{-7}	3.98^{-5}	3.98^{-3}
2.00^{3}	1.65^{-12}	2.78^{-12}	1.14^{-11}	2.64^{-10}	2.21^{-8}	2.20^{-6}	2.20^{-4}
5.00^{3}	7.57^{-13}	9.60^{-13}	1.92^{-12}	1.25^{-11}	4.60^{-10}	3.95^{-8}	3.94^{-6}
1.00^{4}	4.39^{-13}	4.97^{-13}	7.27^{-13}	2.22^{-12}	2.88^{-11}	1.31^{-9}	1.28^{-7}
2.00^{4}	2.57^{-13}	2.73^{-13}	3.32^{-13}	6.08^{-13}	2.72^{-12}	8.82^{-11}	8.62^{-9}
5.00^{4}	1.24^{-13}	1.27^{-13}	1.36^{-13}	1.71^{-13}	3.33^{-13}	8.65^{-12}	8.40^{-10}
1.00^{5}	6.97^{-14}	7.02^{-14}	7.20^{-14}	7.84^{-14}	1.12^{-13}	2.38^{-12}	2.29^{-10}
2.00^{5}	3.75^{-14}	3.75^{-14}	3.77^{-14}	3.81^{-14}	4.53^{-14}	7.46^{-13}	7.08^{-11}
5.00^{5}	1.54^{-14}	1.53^{-14}	1.52^{-14}	1.47^{-14}	1.54^{-14}	1.77^{-13}	1.63^{-11}
1.00^{6}	7.36^{-15}	7.34^{-15}	7.27^{-15}	6.96^{-15}	6.90^{-15}	5.84^{-14}	5.21^{-12}
2.00^{6}	3.35^{-15}	3.34^{-15}	3.30^{-15}	3.15^{-15}	3.02^{-15}	1.91^{-14}	1.63^{-12}
5.00^{6}	1.10^{-15}	1.10^{-15}	1.08^{-15}	1.03^{-15}	9.64^{-16}	4.40^{-15}	3.49^{-13}
1.00^{7}	4.51^{-16}	4.49^{-16}	4.40^{-16}	4.22^{-16}	3.92^{-16}	1.53^{-15}	1.16^{-13}

TABLE III

Tabulation of S_{cr} $(cm^3\ s^{-1})$ *for hydrogen* $z = 1$. $N_p = N_e$, $T_p = T_e$, $W = 0$

N_e cm^{-3}	1.00^{8}	1.00^{10}	1.00^{12}	1.00^{14}	1.00^{16}	1.00^{18}	1.00^{20}
T_e K							
5.00^{3}	9.13^{-23}	9.49^{-23}	1.43^{-22}	3.99^{-21}	2.14^{-19}	6.36^{-19}	6.49^{-19}
1.00^{4}	9.57^{-16}	9.82^{-16}	1.30^{-15}	1.36^{-14}	2.71^{-13}	4.28^{-13}	4.31^{-13}
2.00^{4}	3.73^{-12}	3.80^{-12}	4.66^{-12}	2.53^{-11}	1.88^{-10}	2.19^{-10}	2.19^{-10}
5.00^{4}	6.75^{-10}	6.83^{-10}	7.79^{-10}	2.54^{-9}	9.11^{-9}	9.63^{-9}	9.64^{-9}
1.00^{5}	4.39^{-9}	4.43^{-9}	4.87^{-9}	1.25^{-8}	3.47^{-8}	3.60^{-8}	3.60^{-8}
2.00^{5}	1.21^{-8}	1.22^{-8}	1.32^{-8}	2.81^{-8}	6.74^{-8}	6.94^{-8}	6.94^{-8}
5.00^{5}	2.32^{-8}	2.34^{-8}	2.49^{-8}	4.51^{-8}	9.86^{-8}	1.01^{-7}	1.01^{-7}
1.00^{6}	2.83^{-8}	2.86^{-8}	3.02^{-8}	4.93^{-8}	1.04^{-7}	1.07^{-7}	1.07^{-7}
2.00^{6}	2.96^{-8}	2.99^{-8}	3.15^{-8}	4.81^{-8}	9.93^{-8}	1.02^{-7}	1.03^{-7}
5.00^{6}	2.70^{-8}	2.73^{-8}	2.88^{-8}	4.32^{-8}	8.80^{-8}	9.10^{-8}	9.10^{-8}
1.00^{7}	2.33^{-8}	2.36^{-8}	2.51^{-8}	3.99^{-8}	8.37^{-8}	8.66^{-8}	8.66^{-8}

otherwise specified. These results may be compared with the work of several other authors. By simplification of the cascade term, neglect of the radiation field and inclusion of only first neighbour collisions, the statistical balance equations (8) for the highly-excited levels may be replaced by a differential equation (Seaton 1964). This method has limitations in that collisional transitions between more

TABLE IV

Tabulation of α_{cr}/z ($cm^3\ s^{-1}$) *for hydrogenic ion* $z = 4$. $N_p = 0$, $W = 0$, $\rho = N_e/z^7$, $\theta = T_e/z^2$

ρ cm^{-3}	1.00^{8}	1.00^{12}	1.00^{16}	1.00^{20}
θ K				
2.00^{2}	5.86^{-11}	1.73^{-7}	1.73^{-3}	1.73^{1}
5.00^{2}	8.46^{-12}	2.93^{-9}	2.86^{-5}	2.86^{-1}
1.00^{3}	3.36^{-12}	1.86^{-10}	1.53^{-6}	1.53^{-2}
2.00^{3}	1.66^{-12}	1.84^{-11}	7.84^{-8}	7.84^{-4}
5.00^{3}	7.57^{-13}	2.21^{-12}	1.39^{-9}	1.35^{-5}
1.00^{4}	4.40^{-13}	7.60^{-13}	6.12^{-11}	4.63^{-7}
2.00^{4}	2.57^{-13}	3.36^{-13}	4.30^{-12}	2.49^{-8}
5.00^{4}	1.24^{-13}	1.36^{-13}	4.11^{-13}	1.63^{-9}
1.00^{5}	6.97^{-14}	7.20^{-14}	1.23^{-13}	3.46^{-10}
2.00^{5}	3.75^{-14}	3.77^{-14}	4.74^{-14}	9.22^{-11}
5.00^{5}	1.54^{-14}	1.52^{-14}	1.57^{-14}	1.85^{-11}
1.00^{6}	7.37^{-15}	7.27^{-15}	6.93^{-15}	5.49^{-12}
2.00^{6}	3.35^{-15}	3.31^{-15}	3.02^{-15}	1.64^{-12}
5.00^{6}	1.10^{-15}	1.09^{-15}	9.64^{-16}	3.22^{-13}
1.00^{7}	4.51^{-16}	4.46^{-16}	3.91^{-16}	9.26^{-14}

TABLE V

Tabulation of $z^3 S_{cr}$ ($cm^3\ s^{-1}$) *for hydrogenic ion* $z = 4$. $N_p = 0$, $W = 0$, $\rho = N_e/z^7$, $\theta = T_e/z^2$

ρ cm^{-3}	1.00^{8}	1.00^{12}	1.00^{16}	1.00^{20}
θ K				
5.00^{3}	1.53^{-22}	9.78^{-22}	1.62^{-18}	2.20^{-18}
1.00^{4}	1.52^{-15}	4.43^{-15}	1.28^{-12}	1.55^{-12}
2.00^{4}	5.74^{-12}	1.04^{-11}	5.81^{-10}	6.32^{-10}
5.00^{4}	9.90^{-10}	1.31^{-9}	1.80^{-8}	1.87^{-8}
1.00^{5}	6.10^{-9}	7.20^{-9}	5.28^{-8}	5.45^{-8}
2.00^{5}	1.58^{-8}	1.76^{-8}	8.78^{-8}	9.03^{-8}
5.00^{5}	2.81^{-8}	3.02^{-8}	1.12^{-7}	1.15^{-7}
1.00^{6}	3.27^{-8}	3.46^{-8}	1.10^{-7}	1.13^{-7}
2.00^{6}	3.29^{-8}	3.46^{-8}	1.00^{-7}	1.03^{-7}
5.00^{6}	2.88^{-8}	3.02^{-8}	8.05^{-8}	8.38^{-8}
1.00^{7}	2.43^{-8}	2.54^{-8}	6.58^{-8}	6.92^{-8}

distant levels are of importance, while the consistent matching of the low level solution is difficult. The technique has been extended by Hoang-Binh (1968) and Dyson (1969) to include second and third neighbour collisions but this is an incomplete extension and relies on the slow variation of the populations. Sejnowski & Hjellming (1969) have used an iterative method considering a fairly broad band

($\Delta n \sim 20$) of the matrix C (*cf.* equations (9)). Convergence is reportedly slow and this method makes consistent inclusion of the radiation field difficult. Brocklehurst (1970, 1971) has provided fairly extensive tables of population structure in H II regions. He has used the present authors' matrix condensation method, with some differences in cross-section data, and with no explicit inclusion of the radiation field or of proton collisions. Dupree (1972) and Brocklehurst (1973) have given some results for low temperature and low density H I regions. This will be discussed in Section 7.2.

7.1 *Description of population structure*

In illustration of the general behaviour of the populations a series of curves have been constructed for hydrogen under planetary nebula conditions in Figs 4, 5 and 6. A fixed electron density $N_e = 10^4\,cm^{-3}$ and radiation temperature $T_r = 5 \times 10^4\,K$ have been used throughout and proton collisions have been

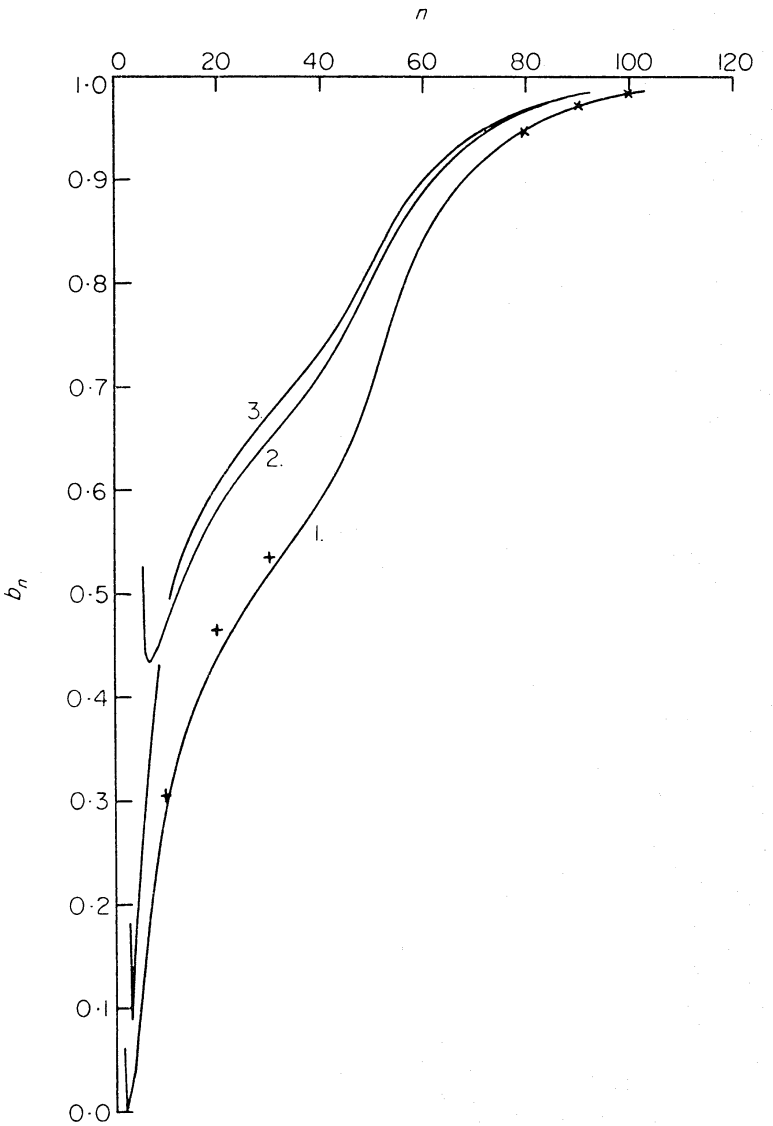

FIG. 4. *H population structure.* $T_e = 5 \times 10^3\,K$, $T_r = 5 \times 10^4\,K$, $N_e = 10^4\,cm^{-3}$, $N_p = 0$. 1, *Case A*, $W = 10^{-20}$, 10^{-16}, 10^{-12}. 2, *Case B*, $W = 10^{-20}$, 10^{-16}. 3, *Case B*, $W = 10^{-12}$. +, *Seaton radiative solution, Case B.* ×, *Hoang-Binh and Dyson, Case B.*

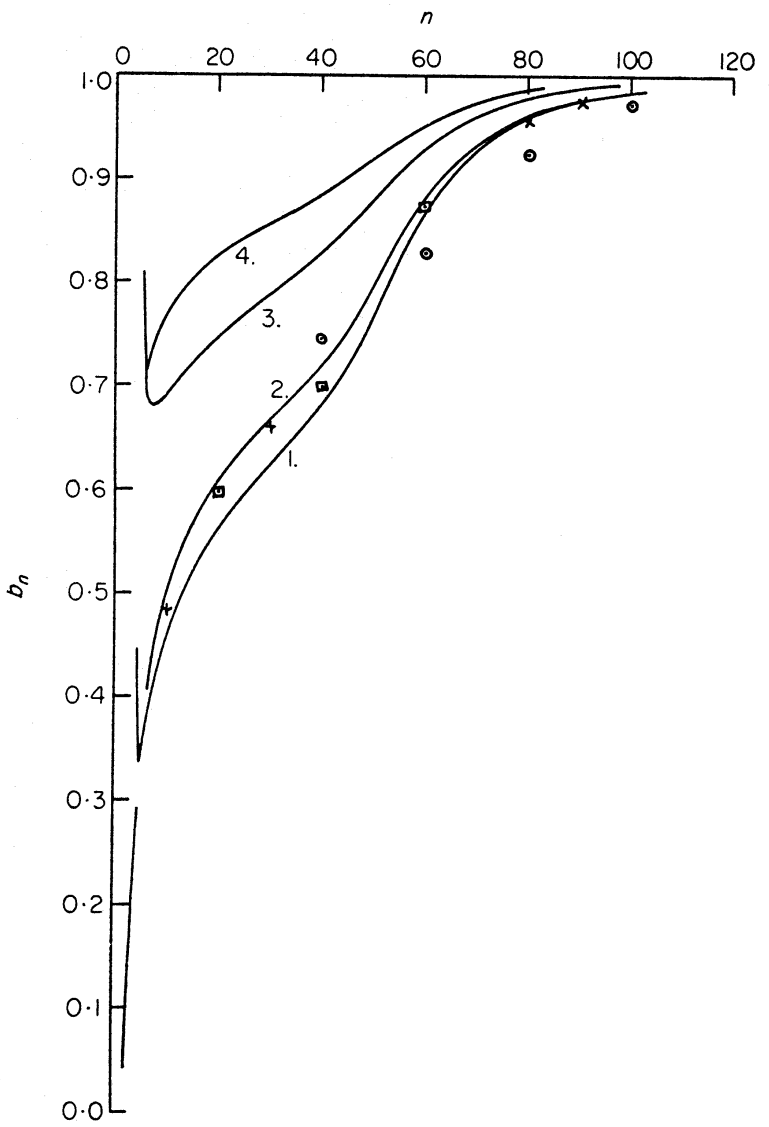

FIG. 5. *H population structure.* $T_e = 10^4\,K$, $T_r = 5 \times 10^4\,K$, $N_e = 10^4\,cm^{-3}$, $N_p = 0$. 1, *Case A*, $W = 10^{-20}$. 2, *Case A*, $W = 10^{-16}$, 10^{-12}. 3, *Case B*, $W = 10^{-20}$, 10^{-16}. 4, *Case B*, $W = 10^{-12}$. +, *Seaton radiative solution, Case B.* ×, *Hoang-Binh and Dyson, Case B.* ⊙, *Seaton, Case B matched to* $b_{40} = 0{\cdot}748$. ⊡, *Sejnowski & Hjellming, Case B.*

neglected; the curves being designed to show the influence of electron temperature and radiation density on the population structure. Both cases A and B of Baker & Menzel (1938) are considered; curves being given for $T_e = 5 \times 10^3$, 10^4 and 2×10^4 K and $W = 10^{-12}$, 10^{-16} and 10^{-20}. More insight can be gained into the behaviour of the curves of Figs 4, 5 and 6 by studying simultaneously Figs 7, 8 and 9. The latter map out the total loss terms A_n due to both collisional and radiative processes from each hydrogenic level n. The effect of variation of electron density is also shown in Figs 7 and 8. The b_n's of the first levels are given in the captions.

Some features of these figures are of interest.

(a) The ground level b_1 varies according to whether it is depleted by photo or collisional excitation and ionization. Thus for curve 3 of Figs 7 and 8 and curve 2 of Fig. 9 at $W = 10^{-12}$ the depletion is by the radiation field, while for curve 1

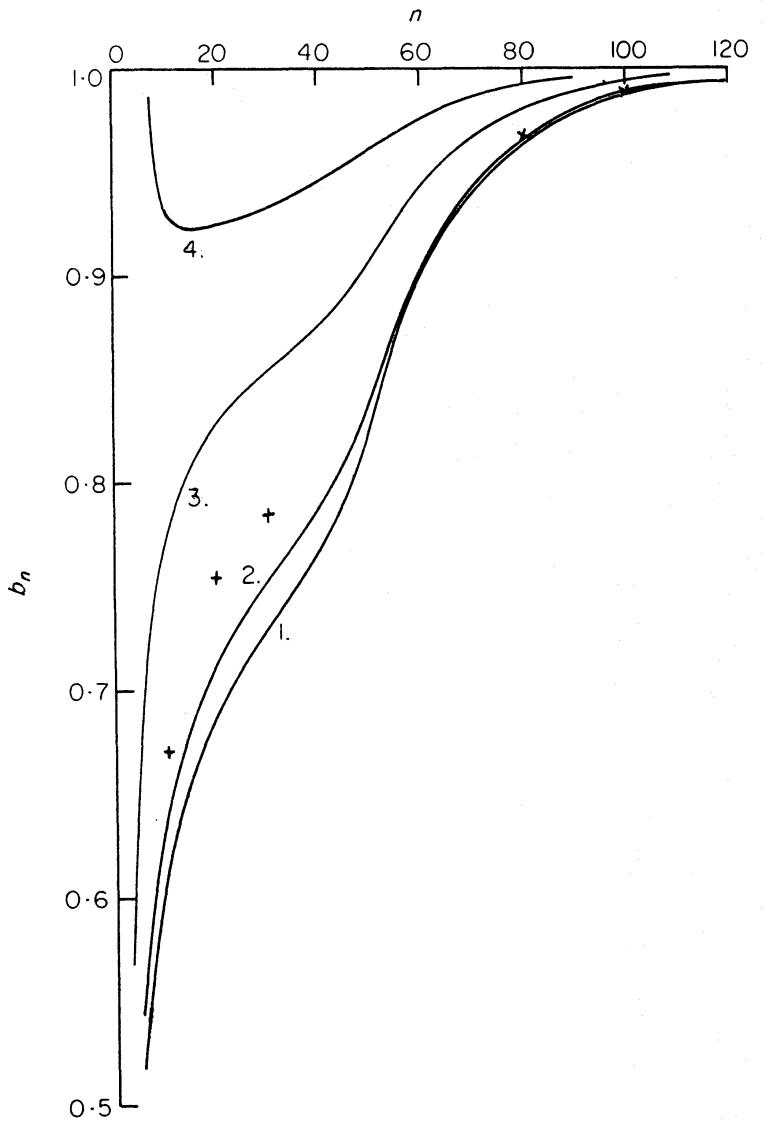

FIG. 6. *H population structure.* $T_e = 2 \times 10^4\,K$, $T_r = 5 \times 10^4\,K$, $N_e = 10^4\,cm^{-3}$, $N_p = 0$. 1, *Case A*, $W = 10^{-20}$. 2, *Case A*, $W = 10^{-16}$. 3, *Case A*, $W = 10^{-12}$. 4, *Case B*, $W = 10^{-20}$, 10^{-16}. *Case B*, $W = 10^{-12}$, $b_n > 1$ *for all* n. +, *Seaton radiative solution, Case B.* ×, *Hoang-Binh and Dyson, Case B.*

of Fig. 9 depletion is by collisions. This also causes the increase in the b_n's for $n = 2$, 3 and 4 by excitation from the ground level. In the present cases the radiation field does not affect the depletion of the excited levels.

(b) The ground level depletion mechanism also influences the highly-excited levels. This is shown by the case A results. In Fig. 4, curve 1, change in the dilution does not affect the b_n's of the higher levels although it has a strong influence on the ground level b_1 (*cf.* Fig. 7). On the other hand in Fig. 5 when the depopulating mechanism of the ground level is changing from collisional to radiative the b_n's increase (*cf.* curves 1 and 2), but stabilize again when the ground level is dilution determined. Fig. 6 follows a similar pattern. This is due to the asymmetric effect of the collisional excitation from the ground level which selectively populates the low levels at the electron temperatures considered here. Since the recombination is entirely radiative, at a given temperature there is a steady flow, say k_1, of electrons

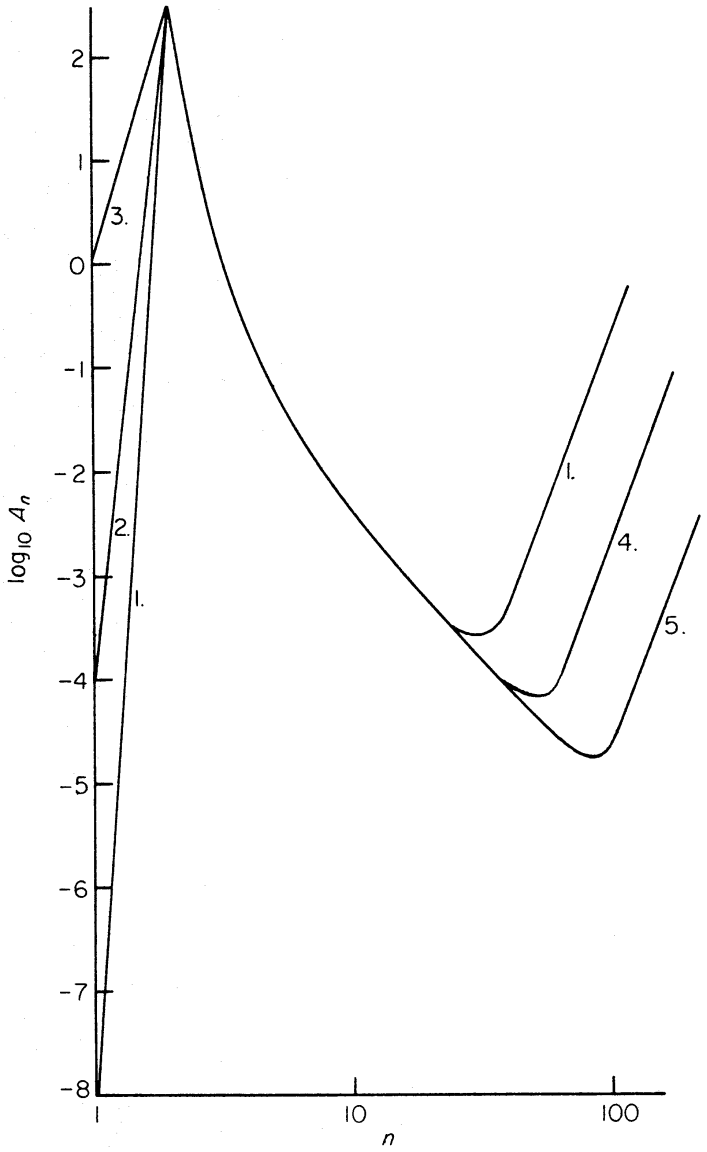

FIG. 7. *H population structure.* A_n *is the rate out of level n.* $T_e = 5 \times 10^3$ *K*, $T_r = 5 \times 10^4$ *K*, $N_p = 0$, *all Case A.* 1, $N_e = 10^4$ *cm*$^{-3}$, $W = 10^{-20}$, $b_1 = 1{\cdot}547^7$. 2, $N_e = 10^4$ *cm*$^{-3}$, $W = 10^{-16}$, $b_1 = 1{\cdot}547^3$. 3, $N_e = 10^4$ *cm*$^{-3}$, $W = 10^{-12}$, $b_1 = 1{\cdot}547^{-1}$. 4, $N_e = 10^2$ *cm*$^{-3}$, $W = 10^{-20}$, 10^{-16}, 10^{-12}. 5, $N_e = 10^0$ *cm*$^{-3}$, $W = 10^{-20}$, 10^{-16}, 10^{-12}.

into the ground level, and k_1 is unaffected by the external radiation field at the dilutions occurring here. The depopulation of the ground level is in general the sum of two components; one dilution dependent, say k_2W, and the other electron density dependent, say k_3N_e. Thus

$$b_1 \propto k_1/(k_2W + k_3N_e). \tag{62}$$

Now the ground population reacts back on the high levels. However, the selection mentioned above means that the ground level influence on the high levels is only dilution dependent, say k_4W. Thus

$$b_n \propto \text{const.} + \frac{k_4k_1W}{k_2W + k_3N_e}. \tag{63}$$

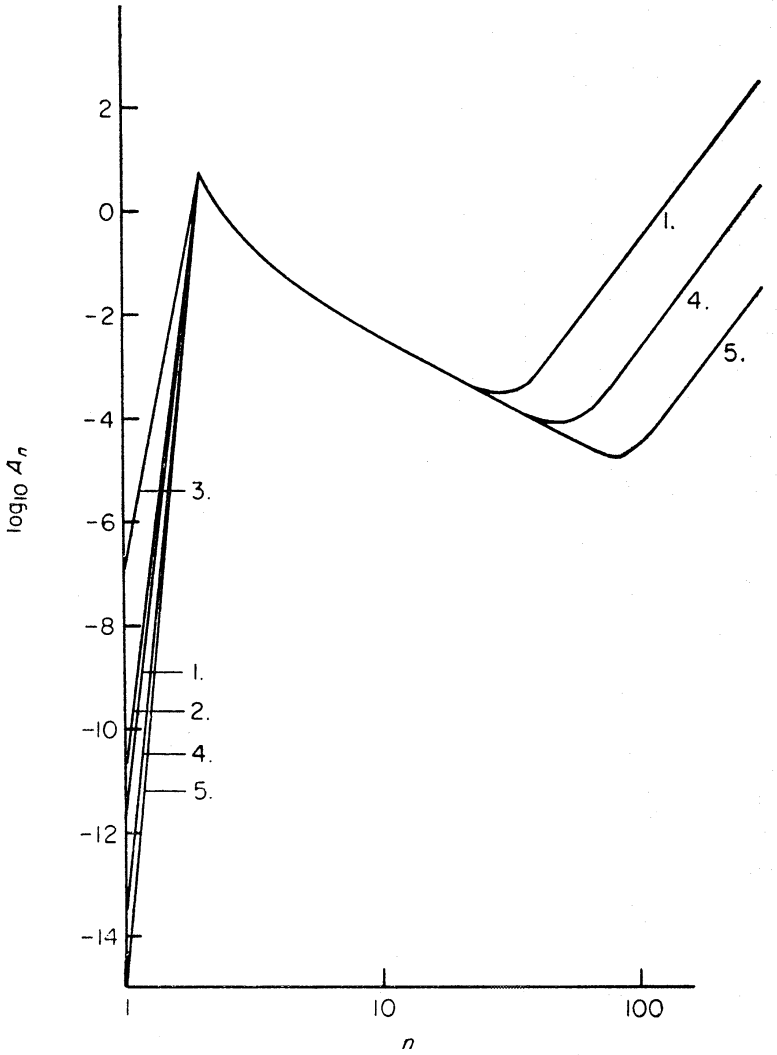

FIG. 8. *H population structure.* A_n *is the rate out of level n.* $T_e = 10^4\,K$, $T_r = 5 \times 10^4\,K$, $N_p = 0$, *all Case A.* 1, $N_e = 10^4\,cm^{-3}$, $W = 10^{-20}$, $b_1 = 1{\cdot}377^{13}$, $b_2 = 5{\cdot}718^{0}$, $b_3 = 3{\cdot}122^{0}$, $b_4 = 1{\cdot}908^{0}$. 2, $N_e = 10^4\,cm^{-3}$, $W = 10^{-16}$, $b_1 = 1{\cdot}919^{10}$. 3, $N_e = 10^4\,cm^{-3}$, $W = 10^{-12}$, $b_1 = 1{\cdot}921^{6}$. 4, $N_e = 10^2\,cm^{-3}$, $W = 10^{-20}$. 5, $N_e = 10^0\,cm^{-3}$, $W = 10^{-20}$.

Thus when the radiation depopulation of the ground level is dominant, there is a constant addition to the b_n's of the high levels independent of dilution (*cf.* Fig. 4, curve 1). When the ground level depopulation is predominantly collisional, there is a reduced addition to the b_n's of the high levels which is dilution dependent (*cf.* Fig. 5, curves 1 and 2; Fig. 6, curves 1, 2 and 3).

(c) In the Baker & Menzel case B, it is assumed that the emission of a Lyman photon is immediately followed by a reabsorption. Thus the first level of the hydrogen atom is effectively removed from the set of interacting levels and the statistical balance equations apply for $n \geq 2$. For consistency this would imply a build-up of electrons in the $n = 2$ level leading to a large over-population for $n = 2$ which would react back on the higher levels. Case B results are shown in Figs 4, 5 and 6 with this assumption. In gaseous nebulae this is probably not the true situation. The degree of build up of the $n = 2$ population depends on the containment of Lyman α in the nebulae. The losses of Lyman α photons (Osterbrock

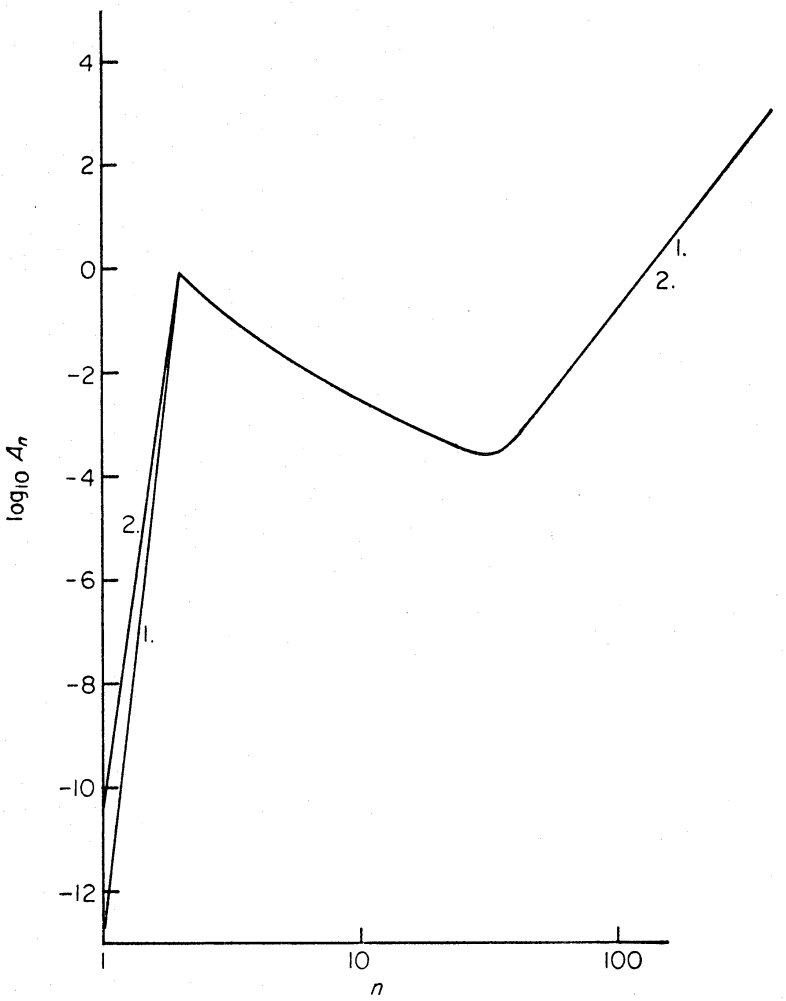

FIG. 9. *H population structure.* A_n *is the rate out of level* n. $T_e = 2 \times 10^4 K$, $T_r = 5 \times 10^4 K$, $N_p = 0$, *all Case A.* 1, $N_e = 10^4\ cm^{-3}$, $W = 10^{-20}$, $b_1 = 1{\cdot}727^{13}$, $b_2 = 7{\cdot}582^0$, $b_3 = 3{\cdot}996^0$, $b_4 = 2{\cdot}458^0$. $W = 10^{-16}$, $b_1 = 1{\cdot}442^{13}$, $b_2 = 6{\cdot}403^0$, $b_3 = 3{\cdot}430^0$, $b_4 = 2{\cdot}159^0$. 2, $N_e = 10^4\ cm^{-3}$, $W = 10^{-12}$, $b_1 = 8{\cdot}745^9$.

1962) by escape from the boundary, by decay of electrons in the $n = 2$ shell (two-photon) or by absorption by dust particles, suggest that the population of the $n = 2$ level cannot grow to such an extent that it influences the higher levels, at least for H II regions not surrounded by an H I region. With a very deep H I region reflection of Lyman α photons back into the H II region may be sufficient to cause more substantial build up of the $n = 2$ population.

(d) Comparison of results with some other sources.

The purely radiative case B solutions (Seaton 1959) for the lower levels have been marked on Figs 4, 5 and 6. The differential equation solution of Seaton (1964) for the high levels at $T_e = 10^4$ K is included in Fig. 5. The results of Dyson (1969) and Hoang-Binh (1968) are almost identical, and are also shown. Results of Sejnowski & Hjellming (1969) are included in Fig. 5. Note that all these results are for case B with a depopulated $n = 2$ level. It can be seen in Fig. 4, curve 1, and Fig. 5, curves 1 and 2, that the Seaton radiative solution for the intermediate levels lies close to the present case A results with a dilution-dependent ground level.

Although the Seaton results describe a depopulated case B, the closeness of the correspondence is not fortuitous but can be shown to arise from the depopulation of the first level being dilution dependent. Thus at $T_e = 5 \times 10^3$ K the situation in Fig. 4, curve 1, corresponds to that of a pure case B radiative solution with depopulated $n = 2$ level, and the Seaton points lie close to curve 1. At $T_e = 10^4$ K there is a slight pumping from the ground level to the higher levels in the present case A solution and so curve 2, Fig. 5, moves to the other side of the Seaton points. At $T_e = 2 \times 10^4$ K there is a much larger excess populating of the high levels due to the ground level pumping and curve 3, Fig. 6, is further above the Seaton points. Note that in Figs 4, 5 and 6 the comparison has been made with the curves in which the depopulating mechanism of the ground level is purely the radiation field. There is good agreement with the b_n's of the very excited levels $n \gtrsim 100$ between curves 1 of Figs 4, 5 and 6 and the results of Hoang-Binh, Dyson and of Sejnowski & Hjellming. Seaton's solution for the b_n's of the very high levels differs more widely from the present results. This is partly due to the fitting to an approximate radiative solution at $n = 40$ which is rather higher than the accurate solution. However, the gradients of the curve also disagree and this arises from the omission of collisions between higher order neighbours, Seaton's curve being steeper than the present results.

7.2 *Discussion of results*

(a) So far consideration has not been given to the influence of proton collisions and the 3 K background radiation on the high level populations. These effects are shown in Table VI. The proton collisions produce some changes, increasing

TABLE VI

Comparison of effects of proton collisions and 3 K radiation on populations. Tabulation of c_n's for hydrogen $z = 1$, $T_p = T_e$, Case A

	$N_e = 10^4$ cm^{-3}, $T_e = 2.00^3$ K			$N_e = 10^4$ cm^{-3}, $T_e = 5.00^3$ K		
n	$W=0, N_p=0$	$W=0, N_p=N_e$ $T_p=T_e$	$W=1, N_p=0$ $T_r=3$ K	$W=0, N_p=0$	$W=0, N_p=N_e$ $T_p=T_e$	$W=1, N_p=0$ $T_r=3$ K
3	1.11737	1.11739	1.11739	1.75094	1.75096	1.75094
5	-8.83209^{-1}	-8.83208^{-1}	-8.83208^{-1}	-7.93600^{-1}	-7.93598^{-1}	-7.93600^{-1}
10	-8.42387^{-1}	-8.42385^{-1}	-8.42385^{-1}	-6.90985^{-1}	-6.90980^{-1}	-6.90983^{-1}
20	-7.08418^{-1}	-7.08414^{-1}	-7.08413^{-1}	-5.57161^{-1}	-5.57148^{-1}	-5.57157^{-1}
50	-3.73882^{-1}	-3.73801^{-1}	-3.73779^{-1}	-2.95942^{-1}	-2.95692^{-1}	-2.95856^{-1}
90	-3.15095^{-2}	-3.14591^{-2}	-3.15120^{-2}	-2.72255^{-2}	-2.70731^{-2}	-2.72255^{-2}
200	-4.15101^{-4}	-4.12493^{-4}	-4.14757^{-4}	-4.07090^{-4}	-4.01543^{-4}	-4.06621^{-4}
300	-4.17631^{-5}	-4.13440^{-5}	-4.16470^{-5}	-4.33939^{-5}	-4.24372^{-5}	-4.32405^{-5}

the coupling between the high levels as expected. It seems therefore that proton collisions should be included in population structure calculations. In a nebula, time scales are sufficiently long for equipartition of energy between electrons and protons and so for the present work on population structure under nebular conditions, it is appropriate to take $T_p = T_e$ and $N_p = N_e$. The 3 K radiation effect is small even though it is a dense radiation field. This is due to the already very strong coupling of the high levels by particle collisions.

TABLE VII

Comparison of effects of zero excitation threshold, finite threshold and Banks et al. (1973) *cross-sections on populations. Tabulation of* Δb_n*'s for hydrogen* $z = 1$.

	$T_e = 2{\cdot}00^2$ K, $N_e = 10^{10}$ cm^{-3}, $N_p = 0$, VR for $s > 3$			$T_e = 2{\cdot}00^2$ K, $N_e = 10^{12}$ cm^{-3}, $N_p = 0$, VR for $s > 3$			$T_e = 2{\cdot}00^2$ K, $N_e = 10^{14}$ cm^{-3}, $N_p = 0$, VR for $s > 3$		
n	Zero IP	Finite IP	PR	Zero IP	Finite IP	PR	Zero IP	Finite IP	PR
6	6.41066^{-10}	1.45517^{-9}	6.66596^{-10}	1.44731^{-7}	2.66016^{-7}	1.37190^{-7}	6.88043^{-7}	7.41193^{-7}	5.29669^{-7}
8	1.95763^{-5}	5.41216^{-5}	2.21661^{-5}	1.55645^{-3}	2.27216^{-3}	1.28873^{-3}	2.04160^{-3}	2.76755^{-3}	1.65493^{-3}
10	4.61212^{-3}	1.00636^{-2}	4.52940^{-3}	3.86055^{-2}	5.10215^{-2}	3.29859^{-2}	4.05535^{-2}	5.26735^{-2}	3.44284^{-2}
12	6.05525^{-2}	8.46736^{-2}	5.63623^{-2}	1.09589^{-1}	1.13593^{-1}	9.94202^{-2}	1.10188^{-1}	1.13486^{-1}	9.99259^{-2}
15	1.27575^{-1}	1.11116^{-1}	1.27631^{-1}	1.09557^{-1}	1.06850^{-1}	1.13432^{-1}	1.08689^{-1}	9.21992^{-2}	1.12798^{-1}
20	4.91171^{-2}	4.33870^{-2}	5.03548^{-2}	3.43155^{-2}	3.43716^{-2}	3.72909^{-2}	3.39402^{-2}	3.41473^{-2}	3.69878^{-2}

Table VIII

Tabulation of b_n's and Δb_n's for hydrogen $z = 1$. Case A, $N_p = N_e$, $T_p = T_e$

$N_e = 10^{-2}$ cm^{-3}, $T_r = 5{\cdot}00^4$ K, $W = 10^{-22}$, $N_p = N_e$, $T_p = T_e$

	$T_e = 5{\cdot}00^1$ K, $N_1/N_+ = 1{\cdot}94^1$		$T_e = 1{\cdot}00^2$ K, $N_1/N_+ = 1{\cdot}23^1$		$T_e = 2{\cdot}00^2$ K, $N_1/N_+ = 7{\cdot}75$		$T_e = 5{\cdot}00^2$ K, $N_1/N_+ = 4{\cdot}31$		$T_e = 1{\cdot}00^3$ K, $N_1/N_+ = 2{\cdot}75$	
n	b_n	Δb_n	b_n	Δb_n	b_n	Δb_n	b_n	Δb_n	b_n	Δb_n
20	1.71^{-5}	8.17^{-5}	9.53^{-4}	7.50^{-4}	1.07^{-2}	3.03^{-3}	6.37^{-2}	7.80^{-3}	1.42^{-1}	1.03^{-2}
30	1.47^{-3}	1.06^{-3}	1.25^{-2}	2.81^{-3}	4.62^{-2}	4.90^{-3}	1.32^{-1}	6.70^{-3}	2.21^{-1}	6.98^{-3}
50	2.14^{-2}	2.05^{-3}	6.09^{-2}	3.12^{-3}	1.21^{-1}	3.71^{-3}	2.23^{-1}	3.84^{-3}	3.11^{-1}	3.59^{-3}
70	5.52^{-2}	1.98^{-3}	1.10^{-1}	2.42^{-3}	1.77^{-1}	2.56^{-3}	2.79^{-1}	2.44^{-3}	3.63^{-1}	2.21^{-3}
90	8.95^{-2}	1.75^{-3}	1.50^{-1}	1.92^{-3}	2.18^{-1}	1.91^{-3}	3.17^{-1}	1.75^{-3}	3.98^{-1}	1.57^{-3}
110	1.20^{-1}	1.60^{-3}	1.83^{-1}	1.64^{-3}	2.51^{-1}	1.58^{-3}	3.47^{-1}	1.41^{-3}	4.24^{-1}	1.25^{-3}
150	1.73^{-1}	1.52^{-3}	2.36^{-1}	1.43^{-3}	3.01^{-1}	1.30^{-3}	3.91^{-1}	1.12^{-3}	4.63^{-1}	9.76^{-4}
200	2.36^{-1}	2.21^{-3}	2.94^{-1}	1.89^{-3}	3.54^{-1}	1.61^{-3}	4.36^{-1}	1.29^{-3}	5.02^{-1}	1.07^{-3}
250	3.41^{-1}	3.79^{-3}	3.83^{-1}	3.26^{-3}	4.28^{-1}	2.78^{-3}	4.96^{-1}	2.22^{-3}	5.51^{-1}	1.83^{-3}
300	5.37^{-1}	4.13^{-3}	5.51^{-1}	3.74^{-3}	5.73^{-1}	3.34^{-3}	6.11^{-1}	2.80^{-3}	6.46^{-1}	2.38^{-3}
350	7.30^{-1}	3.12^{-3}	7.30^{-1}	2.96^{-3}	7.34^{-1}	2.75^{-3}	7.49^{-1}	2.42^{-3}	7.65^{-1}	2.13^{-3}
400	8.59^{-1}	1.91^{-3}	8.54^{-1}	1.87^{-3}	8.52^{-1}	1.80^{-3}	8.54^{-1}	1.65^{-3}	8.59^{-1}	1.49^{-3}

1976MNRAS.174..345B

TABLE VIII—*continued*

$N_e = 10^{-0}$ cm^{-3}, $T_r = 5{\cdot}00^4$ K, $W = 10^{-20}$, $N_p = N_e$, $T_p = T_e$

	$T_e = 5{\cdot}00^1$ K, $N_1/N_+ = 2{\cdot}08^1$		$T_e = 1{\cdot}00^2$ K, $N_1/N_+ = 1{\cdot}27^1$		$T_e = 2{\cdot}00^2$ K, $N_1/N_+ = 7{\cdot}88$		$T_e = 5{\cdot}00^2$ K, $N_1/N_+ = 4{\cdot}34$		$T_e = 1{\cdot}00^3$ K, $N_1/N_+ = 2{\cdot}76$	
n	b_n	Δb_n	b_n	Δb_n	b_n	Δb_n	b_n	Δb_n	b_n	Δb_n
20	1.85^{-5}	8.90^{-5}	9.91^{-4}	7.84^{-4}	1.09^{-2}	3.10^{-3}	6.42^{-2}	7.90^{-3}	1.43^{-1}	1.04^{-2}
30	1.60^{-3}	1.18^{-3}	1.30^{-2}	2.99^{-3}	4.74^{-2}	5.09^{-3}	1.33^{-1}	6.87^{-3}	2.23^{-1}	7.13^{-3}
50	2.38^{-2}	2.37^{-3}	6.46^{-2}	3.44^{-3}	1.26^{-1}	4.01^{-3}	2.27^{-1}	4.08^{-3}	3.15^{-1}	3.80^{-3}
70	6.28^{-2}	2.47^{-3}	1.19^{-1}	2.87^{-3}	1.86^{-1}	2.96^{-3}	2.87^{-1}	2.76^{-3}	3.70^{-1}	2.49^{-3}
90	1.06^{-1}	2.70^{-3}	1.67^{-1}	2.76^{-3}	2.35^{-1}	2.64^{-3}	3.32^{-1}	2.33^{-3}	4.10^{-1}	2.05^{-3}
110	1.57^{-1}	4.69^{-3}	2.18^{-1}	4.30^{-3}	2.83^{-1}	3.82^{-3}	3.73^{-1}	3.19^{-3}	4.47^{-1}	2.71^{-3}
150	3.55^{-1}	8.42^{-3}	3.95^{-1}	7.65^{-3}	4.37^{-1}	6.87^{-3}	5.01^{-1}	5.82^{-3}	5.54^{-1}	5.02^{-3}
200	7.33^{-1}	4.83^{-3}	7.39^{-1}	4.56^{-3}	7.48^{-1}	4.27^{-3}	7.65^{-1}	3.81^{-3}	7.82^{-1}	3.41^{-3}
250	9.04^{-1}	1.90^{-3}	9.04^{-1}	1.86^{-3}	9.05^{-1}	1.80^{-3}	9.08^{-1}	1.67^{-3}	9.13^{-1}	1.55^{-3}
300	9.64^{-1}	6.90^{-4}	9.63^{-1}	6.89^{-4}	9.63^{-1}	6.82^{-4}	9.63^{-1}	6.56^{-4}	9.64^{-1}	6.22^{-4}
350	9.86^{-1}	2.64^{-4}	9.85^{-1}	2.68^{-4}	9.85^{-1}	2.71^{-4}	9.84^{-1}	2.68^{-4}	9.84^{-1}	2.59^{-4}
400	9.94^{-1}	1.09^{-4}	9.94^{-1}	1.12^{-4}	9.94^{-1}	1.15^{-4}	9.93^{-1}	1.17^{-4}	9.93^{-1}	1.15^{-4}

1976MNRAS.174..345B

TABLE VIII—*continued*

$N_e = 10^2$ cm^{-3}, $T_r = 5{\cdot}00^4$ K, $W = 10^{-18}$, $N_p = N_e$, $T_p = T_e$

	$T_e = 5{\cdot}00^1$ K, $N_1/N_+ = 2{\cdot}49^1$		$T_e = 1{\cdot}00^2$ K, $N_1/N_+ = 1{\cdot}41^1$		$T_e = 2{\cdot}00^2$ K, $N_1/N_+ = 8{\cdot}31$		$T_e = 5{\cdot}00^2$ K, $N_1/N_+ = 4{\cdot}42$		$T_e = 1{\cdot}00^3$ K, $N_1/N_+ = 2{\cdot}78$	
n	b_n	Δb_n	b_n	Δb_n	b_n	Δb_n	b_n	Δb_n	b_n	Δb_n
20	2.31^{-5}	1.15^{-4}	1.12^{-3}	9.04^{-4}	1.17^{-2}	3.37^{-3}	6.63^{-2}	8.24^{-3}	1.45^{-1}	1.07^{-2}
30	2.08^{-3}	1.70^{-3}	1.51^{-2}	3.76^{-3}	5.15^{-2}	5.94^{-3}	1.39^{-1}	7.65^{-3}	2.29^{-1}	7.80^{-3}
50	3.42^{-2}	5.32^{-3}	8.07^{-2}	6.51^{-3}	1.44^{-1}	6.87^{-3}	2.46^{-1}	6.50^{-3}	3.32^{-1}	5.84^{-3}
70	1.24^{-1}	1.32^{-2}	1.87^{-1}	1.28^{-2}	2.54^{-1}	1.18^{-2}	3.47^{-1}	1.01^{-2}	4.22^{-1}	8.70^{-3}
90	3.84^{-1}	1.55^{-2}	4.35^{-1}	1.43^{-2}	4.79^{-1}	1.30^{-2}	5.38^{-1}	1.12^{-2}	5.87^{-1}	9.77^{-3}
110	6.74^{-1}	1.05^{-2}	6.99^{-1}	9.57^{-3}	7.19^{-1}	8.77^{-3}	7.46^{-1}	7.70^{-3}	7.68^{-1}	6.83^{-3}
150	9.27^{-1}	2.60^{-3}	9.32^{-1}	2.40^{-3}	9.35^{-1}	2.25^{-3}	9.38^{-1}	2.05^{-3}	9.42^{-1}	1.88^{-3}
200	9.85^{-1}	4.59^{-4}	9.86^{-1}	4.31^{-4}	9.86^{-1}	4.13^{-4}	9.86^{-1}	3.92^{-4}	9.87^{-1}	3.72^{-4}
250	9.96^{-1}	1.04^{-4}	9.96^{-1}	9.87^{-5}	9.96^{-1}	9.66^{-5}	9.96^{-1}	9.47^{-5}	9.96^{-1}	9.22^{-5}
300	9.99^{-1}	2.94^{-5}	9.99^{-1}	2.82^{-5}	9.99^{-1}	2.82^{-5}	9.99^{-1}	2.84^{-5}	9.99^{-1}	2.83^{-5}
350	1.00	9.81^{-6}	1.00	9.58^{-6}	1.00	9.72^{-6}	9.99^{-1}	1.01^{-5}	9.99^{-1}	1.02^{-5}
400	1.00	3.73^{-6}	1.00	3.69^{-6}	1.00	3.82^{-6}	1.00	4.07^{-6}	1.00	4.21^{-6}

TABLE IX

Tabulation of b_n's and Δb_n's for hydrogen $z = 1$. Case B with depopulated $n = 2$ level.
$N_p = N_e$, $T_p = T_e$, $W = 0$

$T_e = 1{\cdot}00^4$ K

	$N_e = 10^4$ cm^{-3}		$N_e = 10^5$ cm^{-3}		$N_e = 10^6$ cm^{-3}		$N_e = 10^7$ cm^{-3}	
n	b_n	Δb_n	b_n	Δb_n	b_n	Δb_n	b_n	Δb_n
3	1.16^{-1}		1.17^{-1}		1.18^{-1}		1.19^{-1}	
4	2.02^{-1}	8.58^{-2}	2.03^{-1}	8.62^{-2}	2.05^{-1}	8.69^{-2}	2.07^{-1}	8.82^{-2}
5	2.77^{-1}	7.50^{-2}	2.78^{-1}	7.54^{-2}	2.81^{-1}	7.62^{-2}	2.85^{-1}	7.76^{-2}
7	3.86^{-1}	4.84^{-2}	3.89^{-1}	4.88^{-2}	3.93^{-1}	4.97^{-2}	4.00^{-1}	5.12^{-2}
10	4.85^{-1}	2.70^{-2}	4.88^{-1}	2.75^{-2}	4.95^{-1}	2.85^{-2}	5.08^{-1}	3.06^{-2}
20	6.25^{-1}	9.03^{-3}	6.36^{-1}	1.14^{-2}	6.69^{-1}	1.96^{-2}	7.75^{-1}	2.56^{-2}
30	6.88^{-1}	6.66^{-3}	7.28^{-1}	1.39^{-2}	8.56^{-1}	1.38^{-2}	9.58^{-1}	7.43^{-3}
50	8.23^{-1}	7.81^{-3}	9.36^{-1}	5.22^{-3}	9.86^{-1}	1.65^{-3}	9.97^{-1}	3.67^{-4}
70	9.48^{-1}	3.05^{-3}	9.87^{-1}	1.00^{-3}	9.98^{-1}	2.15^{-4}	1.00	3.97^{-5}
90	9.84^{-1}	9.15^{-4}	9.96^{-1}	2.23^{-4}	9.99^{-1}	4.28^{-5}	1.00	7.46^{-6}
110	9.94^{-1}	2.92^{-4}	9.99^{-1}	6.33^{-5}	1.00	1.16^{-5}	1.00	1.98^{-6}
150	9.99^{-1}	4.38^{-5}	1.00	8.68^{-6}	1.00	1.53^{-6}	1.00	2.56^{-7}
200	1.00	7.10^{-6}	1.00	1.35^{-6}	1.00	2.34^{-7}	1.00	3.88^{-8}
250	1.00	1.70^{-6}	1.00	3.19^{-7}	1.00	5.47^{-8}	1.00	9.02^{-9}
300	1.00	5.22^{-7}	1.00	9.67^{-8}	1.00	1.65^{-8}	1.00	2.72^{-9}
350	1.00	1.91^{-7}	1.00	3.53^{-8}	1.00	6.02^{-9}	1.00	9.88^{-10}
400	1.00	8.01^{-8}	1.00	1.47^{-8}	1.00	2.50^{-9}	1.00	4.11^{-10}

TABLE IX—*continued*

$T_e = 2{\cdot}00^4$ K

	$N_e = 10^4$ cm^{-3}		$N_e = 10^5$ cm^{-3}		$N_e = 10^6$ cm^{-3}		$N_e = 10^7$ cm^{-3}	
n	b_n	Δb_n	b_n	Δb_n	b_n	Δb_n	b_n	Δb_n
3	4.23^{-1}		4.23^{-1}		4.25^{-1}		4.27^{-1}	
4	4.85^{-1}	6.18^{-2}	4.85^{-1}	6.20^{-2}	4.87^{-1}	6.24^{-2}	4.90^{-1}	6.30^{-2}
5	5.41^{-1}	5.65^{-2}	5.42^{-1}	5.67^{-2}	5.44^{-1}	5.71^{-2}	5.47^{-1}	5.78^{-2}
7	6.17^{-1}	3.32^{-2}	6.19^{-1}	3.34^{-2}	6.22^{-1}	3.39^{-2}	6.27^{-1}	3.47^{-2}
10	6.82^{-1}	1.75^{-2}	6.84^{-1}	1.77^{-2}	6.89^{-1}	1.83^{-2}	6.97^{-1}	1.96^{-2}
20	7.70^{-1}	5.58^{-3}	7.77^{-1}	6.95^{-3}	7.97^{-1}	1.18^{-2}	8.61^{-1}	1.56^{-2}
30	8.09^{-1}	3.97^{-3}	8.33^{-1}	8.28^{-3}	9.09^{-1}	8.45^{-3}	9.73^{-1}	4.61^{-3}
50	8.89^{-1}	4.72^{-3}	9.58^{-1}	3.29^{-3}	9.90^{-1}	1.07^{-3}	9.98^{-1}	2.46^{-4}
70	9.66^{-1}	1.94^{-3}	9.91^{-1}	6.60^{-4}	9.98^{-1}	1.47^{-4}	1.00	2.79^{-5}
90	9.89^{-1}	6.04^{-4}	9.98^{-1}	1.51^{-4}	1.00	3.00^{-5}	1.00	5.40^{-6}
110	9.96^{-1}	1.98^{-4}	9.99^{-1}	4.40^{-5}	1.00	8.30^{-6}	1.00	1.46^{-6}
150	9.99^{-1}	3.02^{-5}	1.00	6.13^{-6}	1.00	1.11^{-6}	1.00	1.92^{-7}
200	1.00	4.93^{-6}	1.00	9.60^{-7}	1.00	1.71^{-7}	1.00	2.93^{-8}
250	1.00	1.18^{-6}	1.00	2.25^{-7}	1.00	3.98^{-8}	1.00	6.79^{-9}
300	1.00	3.64^{-7}	1.00	6.89^{-8}	1.00	1.21^{-8}	1.00	2.06^{-9}
350	1.00	1.33^{-7}	1.00	2.51^{-8}	1.00	4.40^{-9}	1.00	7.47^{-10}
400	1.00	5.56^{-8}	1.00	1.04^{-8}	1.00	1.82^{-9}	1.00	3.09^{-10}

TABLE IX—*continued*

$T_e = 5{\cdot}00^4$ K

	$N_e = 10^4$ cm^{-3}		$N_e = 10^5$ cm^{-3}		$N_e = 10^6$ cm^{-3}		$N_e = 10^7$ cm^{-3}	
n	b_n	Δb_n	b_n	Δb_n	b_n	Δb_n	b_n	Δb_n
3	1.15		1.15		1.15		1.15	
4	1.00	-1.50^{-1}	1.00	-1.50^{-1}	1.00	-1.50^{-1}	1.00	-1.50^{-1}
5	9.70^{-1}	-3.21^{-2}	9.70^{-1}	-3.21^{-2}	9.70^{-1}	-3.20^{-2}	9.71^{-1}	-3.20^{-2}
7	9.57^{-1}	-3.00^{-3}	9.57^{-1}	-2.97^{-3}	9.58^{-1}	-2.92^{-3}	9.59^{-1}	-2.81^{-3}
10	9.58^{-1}	8.97^{-4}	9.58^{-1}	9.31^{-4}	9.59^{-1}	1.01^{-3}	9.60^{-1}	1.17^{-3}
20	9.67^{-1}	7.43^{-4}	9.68^{-1}	9.14^{-4}	9.71^{-1}	1.57^{-3}	9.80^{-1}	2.14^{-3}
30	9.73^{-1}	5.53^{-4}	9.76^{-1}	1.13^{-3}	9.86^{-1}	1.23^{-3}	9.96^{-1}	6.89^{-4}
50	9.84^{-1}	6.61^{-4}	9.93^{-1}	4.97^{-4}	9.98^{-1}	1.71^{-4}	1.00	4.06^{-5}
70	9.95^{-1}	2.90^{-4}	9.99^{-1}	1.04^{-4}	1.00	2.42^{-5}	1.00	4.77^{-6}
90	9.98^{-1}	9.35^{-5}	1.00	2.44^{-5}	1.00	5.02^{-6}	1.00	9.36^{-7}
110	9.99^{-1}	3.09^{-5}	1.00	7.10^{-6}	1.00	1.39^{-6}	1.00	2.53^{-7}
150	1.00	4.77^{-6}	1.00	9.95^{-7}	1.00	1.87^{-7}	1.00	3.35^{-8}
200	1.00	7.74^{-7}	1.00	1.55^{-7}	1.00	2.86^{-8}	1.00	5.07^{-9}
250	1.00	1.83^{-7}	1.00	3.60^{-8}	1.00	6.59^{-9}	1.00	1.16^{-9}
300	1.00	5.55^{-8}	1.00	1.08^{-8}	1.00	1.97^{-9}	1.00	3.47^{-10}
350	1.00	2.01^{-8}	1.00	3.90^{-9}	1.00	7.09^{-10}	1.00	1.25^{-10}
400	1.00	8.33^{-9}	1.00	1.61^{-9}	1.00	2.92^{-10}	1.00	5.12^{-11}

(b) At low temperatures, the threshold behaviour of the cross-sections becomes important. As discussed in Section 4.3, there should be a finite threshold law for the cross-sections. Use of the finite electron–hydrogenic ion threshold demonstrates the sort of variation produced in populations. At temperatures $T_e \sim 200$ K neighbouring transitions for levels with principal quantum number ~ 20 are affected provided the electron density is sufficiently high. The effect is shown and contrasted with the use of PR cross-sections for $s \leq 3$ in Table VII.

(c) Application of population structure calculations to H I regions has been considered previously by Dupree (1972) and by Brocklehurst (1973). The results of Dupree are unreliable since the cross-sections used were much too large (*cf.* Percival & Seaton 1972) and the calculation of the populations rather approximate. Results are given in Table VIII of the b_n's and Δb_n's of hydrogen at a series of temperatures and densities relevant to low temperature and low density H I regions with $N_p = N_e$ and $T_p = T_e$. The radiation field is assumed to be that of a very dilute stellar radiation field at varying dilutions and $T_r = 5 \times 10^4$ K. The principal effect of the radiation field in the H I region is to determine the rate of ionization from the ground level. Variation of the dilution of the radiation field affects the ground level and has only a small effect on the high level populations at the densities considered. Brocklehurst considers the effect of the thermal continuum from a neighbouring H II region.

(d) In H II regions, depopulated case B results have been given by Brocklehurst (1970, 1971) over a wide range of values of T_e and N_e. In Table IX results are given applying to compact H II regions which are not given by Brocklehurst's results. Case B is assumed with a depopulated $n = 2$ level, and proton collisions are included with $N_p = N_e$ and $T_p = T_e$.

(e) The calculations given here are illustrative and do not cover complete ranges of parameters. FORTRAN programs are available which will produce results for other conditions of interest.

ACKNOWLEDGMENTS

This research was supported by a Science Research Council grant. We wish to thank A. W. Stewart for his computational assistance.

REFERENCES

Alder, K., Bohr, A., Huus, T., Mottelson, B. & Winther, A., 1956. *Rev. mod. Phys.*, **28**, 432.
Baker, J. G. & Menzel, D. H., 1938. *Astrophys. J.*, **88**, 52.
Banks, D., Percival, I. C. & Richards, D., 1973. *Astrophys. Lett.*, **14**, 161.
Bates, D. R., Kingston, A. E. & McWhirter, R. W. P., 1962. *Proc. R. Soc.*, **A267**, 297.
Brocklehurst, M., 1970. *Mon. Not. R. astr. Soc.*, **148**, 417.
Brocklehurst, M., 1971. *Mon. Not. R. astr. Soc.*, **153**, 471.
Brocklehurst, M., 1973. *Astrophys. Lett.*, **14**, 81.
Burgess, A., 1958. *Mon. Not. R. astr. Soc.*, **118**, 477.
Burgess, A., 1964a. *Astrophys. J.*, **139**, 776.
Burgess, A., 1964b. *Proceedings of the symposium on atomic collision processes in plasmas*, Culham, UKAEA (Rep. **4818**, 63).
Burgess, A. & Percival, I. C., 1968. *Adv. atom. molec. Phys.*, **4**, 109.
Burgess, A. & Summers, H. P., 1969. *Astrophys. J.*, **157**, 1007.
D'Angelo, N., 1961. *Phys. Rev.*, **121**, 505.
D'Angelo, N., 1965. *Phys. Rev.*, **140A**, 1488.
Dupree, A. K., 1972. *Astrophys. J.*, **173**, 293.

Dyson, J. E., 1969. *Astrophys. J.*, **155,** 47.
Grysinski, M., 1959. *Phys. Rev.*, **115,** 374.
Hinnov, E. & Hirschberg, J. G., 1962. *Phys. Rev.*, **125,** 795.
Hoang-Binh, D., 1968. *Astrophys. Lett.*, **2,** 231.
Karzas, W. J. & Latter, R., 1961. *Astrophys. J. Suppl.*, **6,** 167.
Menzel, D. H. & Baker, J. G., 1937. *Astrophys. J.*, **86,** 70.
Menzel, D. H. & Pekeris, C. L., 1935. *Mon. Not. R. astr. Soc.*, **96,** 77.
Osterbrock, D. E., 1962. *Astrophys. J.*, **135,** 195.
Pengelly, R. M. & Seaton, M. J., 1964. *Mon. Not. R. astr. Soc.*, **127,** 165.
Percival, I. C. & Richards, D., 1970. *J. Phys. B.*, **3,** 1035.
Percival, I. C. & Richards, D., 1971a. *J. Phys. B.*, **4,** 918.
Percival, I. C. & Richards, D., 1971b. *J. Phys. B.*, **4,** 932.
Percival, I. C. & Seaton, M. J., 1972. *Astrophys. Lett.*, **11,** 31.
Richards, D., 1973. *J. Phys. B.*, **6,** 823.
Seaton, M. J., 1955. *Proc. Phys. Soc.*, **68A,** 457.
Seaton, M. J., 1959. *Mon. Not. R. astr. Soc.*, **119,** 81.
Seaton, M. J., 1962. *Proc. Phys. Soc.*, **79,** 1105.
Seaton, M. J., 1964. *Mon. Not. R. astr. Soc.*, **127,** 117.
Sejnowski, T. J. & Hjellming, R. M., 1969. *Astrophys. J.*, **156,** 915.
Thomson, J. J., 1912. *Phil. Mag.*, **23,** 449.
Van Regemorter, H., 1962. *Astrophys. J.*, **136,** 906.

APPENDIX A

EVALUATION OF $g_{nn'}{}^{\mathrm{I}}$

The analytic form for $g_{nn'}{}^{\mathrm{I}}$ has been given by Menzel & Pekeris (1935). This is

$$g_{nn'}{}^{\mathrm{I}} = \frac{\pi\sqrt{3}[(n-n')/(n+n')]^{2n+2n'}\, nn'}{(n-n')}\,|\Delta(n,n')| \qquad \text{(A1)}$$

where

$$\Delta(n,n') = \left[{}_2F_1\left(-n+1,\ -n';\ 1;\ \frac{-4nn'}{(n-n')^2}\right)\right]^2 - \left[{}_2F_1\left(-n'+1,\ -n;\ 1;\ \frac{-4nn'}{(n-n')^2}\right)\right]^2$$

and the ${}_2F_1$ are hypergeometric functions.

It is necessary to evaluate $g_{nn'}{}^{\mathrm{I}}$ rapidly for $1 \le n' < n \lesssim 1000$ in typical computations and so it is important to replace formula (A1) by a simpler expression. When n'/n is small and n' large an asymptotic expansion for $g_{nn'}{}^{\mathrm{I}}$ can be obtained by the method of steepest descents (Menzel & Pekeris 1935; Burgess 1958). This is

$$g_{nn'}{}^{\mathrm{I}} \sim 1 - \frac{0{\cdot}1728[1+(n'/n)^2]}{[1-(n'/n)^2]^{2/3}\, n'^{2/3}} - \frac{0{\cdot}0496([1-\frac{4}{3}(n'/n)^2+(n'/n)^4]}{[1-(n'/n)^2]^{4/3}\, n'^{4/3}} + \ldots \qquad \text{(A2)}$$

When $n' = 1$ and n varies the expression for $g_{nn'}{}^{\mathrm{I}}$ is particularly simple

$$g_{nn'}{}^{\mathrm{I}} = \pi\sqrt{3}\left(\frac{n-1}{n+1}\right)^{2n+2} \frac{n}{n-1}\left|-\frac{8n}{(n-1)} + \frac{16n^2}{(n-1)^2}\right|. \qquad \text{(A3)}$$

A suitable fit along $n' = n-1$ is

$$g_{n,n-1}{}^{\mathrm{I}} \simeq 0{\cdot}778 - \frac{0{\cdot}1554}{n^2} - \frac{0{\cdot}370}{n^4}. \qquad \text{(A4)}$$

From the asymptotic expansion for n'/n small and n large, as n' increases $g_{nn'}{}^{\mathrm{I}}$ increases towards the value 1 like $1 - a/n'^{2/3}$. Further, fitting along the line $2n' = n$ and interpolating between these values using the behaviour with respect to n' gives

the following expansion

$$g_{nn'}{}^{\mathrm{I}} \simeq 1{\cdot}0 - T_4(T_1G_1 + T_2G_2 + T_3G_3) \tag{A5}$$

where, for $n' < n$,

$$G_1 = \left(0{\cdot}203 + \frac{0{\cdot}256}{n^2} + \frac{0{\cdot}257}{n^4}\right) n$$

$$G_2 = 0{\cdot}170n + 0{\cdot}18$$

$$G_3 = \left(0{\cdot}2214 + \frac{0{\cdot}1554}{n^2} + \frac{0{\cdot}370}{n^4}\right) n$$

$$T_1 = (2n' - n)(n' - n + 1)$$

$$T_2 = 4{\cdot}0(n' - 1)(n - n' - 1)$$

$$T_3 = (2n' - n - 0{\cdot}001)(n' - 0{\cdot}999)$$

$$T_4 = \frac{1}{(n - 1{\cdot}999)^2} \frac{1}{nn'^{2/3}} \left(\frac{n-1}{n-n'}\right)^{2/3}.$$

Comparison of (A5) with the exact evaluation of (A1) shows that the approximate expression is accurate to within 0·5 per cent for all n and n' (N. B. $g_{nn'}{}^{\mathrm{I}} = g_{n'n}{}^{\mathrm{I}}$).

APPENDIX B

EVALUATION OF $g_{i\kappa,n}{}^{\mathrm{II}}$

The analytic form for $g_{i\kappa,n}{}^{\mathrm{II}}$ has been given by Menzel & Pekeris (1935).

$$g_{i\kappa,n}{}^{\mathrm{II}} = \frac{\pi\sqrt{3}\kappa n \exp\left[-4\kappa \tan^{-1}(n/\kappa)\right]}{(\kappa^2 + n^2)^{1/2}\left[1 - \exp\left(-2\pi\kappa\right)\right]} \left|\Delta(i\kappa, n)\right| \tag{B1}$$

where

$$\Delta(i\kappa, n) = \left[{}_2F_1\left(-i\kappa + 1, -n; 1; \frac{-4i\kappa n}{(i\kappa - n)^2}\right)\right]^2 - \left[{}_2F_1\left(-n + 1, -i\kappa; 1; \frac{-4i\kappa n}{(i\kappa - n)^2}\right)\right]^2.$$

$g_{i\kappa,n}{}^{\mathrm{II}}$ has been evaluated for a wide range of values of κ and n by Karzas & Latter (1959). As in the case of $g_{nn'}{}^{\mathrm{I}}$ it is advantageous to have a simple approximate expression for $g_{i\kappa,n}{}^{\mathrm{II}}$. For large κ, that is close to the ionization threshold, an asymptotic expansion is again available (Menzel & Pekeris 1935; Burgess 1958)

$$g_{i\kappa,n}{}^{\mathrm{II}} \sim 1 - \frac{0{\cdot}1728(1 - n^2/\kappa^2)}{(1 + n^2/\kappa^2)^{2/3}\, n^{2/3}} - \frac{0{\cdot}0496\left[1 + \frac{4}{3}(n^2/\kappa^2) + n^4/\kappa^4\right]}{(1 + n^2/\kappa^2)^{4/3}\, n^{4/3}} \tag{B2}$$

valid for $n/\kappa \ll 1$ and n large. As is to be expected $g_{i\infty,n}{}^{\mathrm{II}} = g_{\infty,n}{}^{\mathrm{I}}$. However, the asymptotic expansion has incorrect behaviour for κ small. Directly from equation (B1), $g_{i\kappa,n}{}^{\mathrm{II}} \sim 4\sqrt{3}\kappa$ as $\kappa \to 0$, independent of n. This behaviour can be obtained by modification of (B2). A suitable approximate expression is

$$g_{i,\kappa n}{}^{\mathrm{II}} \simeq 1{\cdot}0 \Bigg/ \left\{1 - \frac{4}{3}\frac{0{\cdot}1728(u-1)}{n^{2/3}(u+1)^{2/3}} + \left(\frac{28}{18}\left[\frac{0{\cdot}1728(u-1)}{n^{2/3}(u+1)^{2/3}}\right]^2 + \frac{4}{3}\left[\frac{0{\cdot}0496(u^2 + \frac{4}{3}u + 1)}{n^{4/3}(u+1)^{4/3}}\right]\right)\right\}^{3/4} \tag{B3}$$

where $u = n^2/\kappa^2$. As $u \to \infty$ (or $\kappa \to 0$), this is $\sim 5{\cdot}3\,\kappa$ which is roughly the correct

behaviour for small κ. Up to terms in $1/n^{4/3}$ (B3) yields (B2) which is the correct asymptotic form for n/κ small and n large. Also expression (B3) is quite satisfactory for $n \geq 1$. Generally over all ranges of κ and n of relevance for this work, expression (B3) is accurate to $\sim 0{\cdot}5$ per cent.

APPENDIX C

IMPACT PARAMETER CROSS-SECTIONS FOR ELECTRON AND PROTON IMPACT

Treating the colliding particle as a time-dependent perturbation, the probability of the transition from state n to n' is

$$P_{n\to n'} = \frac{1}{\hbar^2}\left|\int_{-\infty}^{\infty} u_{nn'}(t)\exp(ipt)\,dt\right|^2 \tag{C1}$$

where $u_{nn'}$ is the matrix element of the interaction energy between states n and n' and $p = \Delta E_{nn'}/\hbar$. If the trajectory of the colliding particle is $\boldsymbol{r}'(t)$ then considering only the long range dipole part of the interaction energy,

$$P_{n\to n'} = \frac{e^4}{\hbar^2}\frac{\mathscr{R}_{n'n}}{3\omega_n}\left|\int_{-\infty}^{\infty}\exp(ipt)\frac{\boldsymbol{r}'(t)}{r'^3(t)}\,dt\right|^2. \tag{C2}$$

ω_n is the statistical weight of the initial state and $(1/3\omega_n)\,\mathscr{R}_{n'n} = (I_{\mathrm{H}}/\Delta E_{n'n})\,f_{n\to n'}$ where $f_{n\to n'}$ is the oscillator strength.

Integrating $P_{n\to n'}$ over all possible trajectories for the colliding particle yields the cross-section

$$Q_{n\to n'} = \int_0^{\infty} P_{n\to n'}(R_i)\,2\pi R_i\,dR_i \tag{C3}$$

where R_i is the impact parameter.

Let the target ion have charge Ze; then for a colliding electron with velocity V at ∞, assuming that the trajectory is in the x–y plane symmetrical about the x-axis

$$\frac{1}{r'} = \frac{1}{a(\epsilon^2-1)}(1+\epsilon\cos\theta)$$

where

$$a = \frac{Ze^2}{mV^2}, \qquad \epsilon = \sqrt{1+\frac{m^2V^2R_i^2}{Z^2e^4}}. \tag{C4}$$

It is convenient to use the parametric coordinate ω so that

$$r' = a(\epsilon\cosh\omega - 1), \qquad t = \frac{a}{V}(\epsilon\sinh\omega - \omega) \tag{C5}$$

$$\begin{aligned} I_{x'} &= \int_{-\infty}^{\infty}\exp(ipt)\frac{x'}{r'^3}\,dt \\ &= \frac{\exp(\pi\xi/2)}{aV}\int_{-\infty}^{\infty}\exp(-\xi\epsilon\cosh\omega - i\xi\omega)\frac{\epsilon - i\sinh\omega}{(i\epsilon\sinh\omega - 1)^2}\,d\omega \\ &= \frac{\xi\exp(\pi\xi/2)}{aV}\int_{-\infty}^{\infty}\exp(-\xi\epsilon\cosh\omega - i\xi\omega)\cosh\omega\,d\omega \\ &= -\frac{\xi\exp(\pi\xi/2)}{aV}\frac{\partial}{\partial(\xi\epsilon)}\int_{-\infty}^{\infty}\exp(-\xi\epsilon\cosh\omega - i\xi\omega)\,d\omega \\ &= -\frac{2\xi\exp(\pi\xi/2)}{aV}K_{i\xi}'(\xi\epsilon) \end{aligned} \tag{C6}$$

where

$$\xi = \frac{pa}{V} = \frac{\Delta E_{nn'}}{\hbar}\frac{a}{V}$$

and K is a modified Bessel function. Similarly

$$\begin{aligned} I_{y'} &= \int_{-\infty}^{\infty} \exp(ipt)\frac{r'\sin\theta}{r'^3}\,dt \\ &= \frac{\sqrt{\epsilon^2-1}}{aV}\int_{-\infty}^{\infty}\exp[i\xi(\epsilon\sinh\omega-\omega)]\frac{\sinh\omega}{(\epsilon\cosh\omega-1)^2}\,d\omega \qquad \text{(C7)} \\ &= \frac{\sqrt{\epsilon^2-1}}{aV}\exp(\pi\xi/2)\frac{\xi}{\epsilon}\int_{-\infty}^{\infty}\exp(-\xi\epsilon\cosh\omega-i\xi\omega)\,d\omega \\ &= \frac{2i\sqrt{\epsilon^2-1}}{aV}\exp(\pi\xi/2)\frac{\xi}{\epsilon}K_{i\xi}(\xi\epsilon). \end{aligned}$$

Further, since

$$R_i\,dR_i = a^2\epsilon\,d\epsilon = \frac{a^2}{\xi^2}(\epsilon\xi)\,d(\epsilon\xi),$$

$$2\pi\int|I_{x'}{}^2+I_{y'}{}^2|\,R_i\,dR_i = \frac{8\pi}{V^2}\exp(\pi\xi)\,[K_{i\xi}(\xi\epsilon)\,K_{i\xi}{}'(\xi\epsilon)\,\xi\epsilon]. \qquad \text{(C8)}$$

From reciprocity it is required that $P_{n\to n'} = P_{n'\to n}$. This is achieved by suitably symmetrizing;

$$\begin{aligned} \xi = \frac{pa}{V} = \frac{\Delta E_{nn'}}{\hbar}\frac{Ze^2}{mV^3} &\xrightarrow{\text{sym}} \frac{Z}{a_0}\left|\frac{1}{k_n}-\frac{1}{k_{n'}}\right| \\ \delta = \xi\epsilon-\xi = \frac{\xi}{a}R^{\mathrm{c}} = \frac{\Delta E_{nn'}}{\hbar V}R^{\mathrm{c}} &\xrightarrow{\text{sym}} R^{\mathrm{c}}|k_n-k_{n'}|, \qquad \text{(C9)} \end{aligned}$$

where R^{c} is the distance of closest approach and k_n and $k_{n'}$ are the initial and final wave numbers of the colliding electron.

$$\frac{4e^4}{\hbar^2a^2V^2\epsilon^2} = \frac{4e^4m^2V^2}{\hbar^4V^4(R^{\mathrm{c}}+Ze^2/mV^2)^2} \xrightarrow{\text{sym}} \frac{4k_nk_{n'}}{a_0{}^2(k_nk_{n'}R^{\mathrm{c}}+Z/a_0)^2}. \qquad \text{(C10)}$$

Therefore

$$P_{n\to n'} = 4\left(\frac{I_{\mathrm{H}}}{\Delta E_{nn'}}f_{n\to n'}\right)\frac{k_nk_{n'}}{(k_nk_{n'}R^{\mathrm{c}}+Z/a_0)^2}\exp(\pi\xi)\,(\xi\epsilon)^2 \times\left[K_{i\xi}{}'^2(\xi\epsilon)+\frac{\epsilon^2-1}{\epsilon^2}K_{i\xi}{}^2(\xi\epsilon)\right]. \qquad \text{(C11)}$$

Write

$$P_{n\to n'} = 4\left(\frac{I_{\mathrm{H}}}{\Delta E_{nn'}}f_{n\to n'}\right)\frac{k_nk_{n'}}{(k_nk_{n'}R^{\mathrm{c}}+Z/a_0)^2}X(\xi,\delta). \qquad \text{(C12)}$$

The condition for strong coupling is given by the solution $\delta_1(\delta_1 = R_1{}^{\mathrm{c}}|k_n-k_{n'}|)$ of $2P_{n\to n'} = 1$. Then

$$\tfrac{1}{2}\pi R_1{}^2 = \frac{I_{\mathrm{H}}}{W_n}\left[\tfrac{1}{2}k_nk_{n'}(R_1{}^{\mathrm{c}})^2+\frac{Z}{a_0}R_1{}^{\mathrm{c}}\right]\pi a_0{}^2 \qquad \text{(C13)}$$

TABLE CI

Tabulation of $X(\xi, \delta)$

δ	ξ 0.0	0.1	0.2	0.3	0.4	0.5	0.6
0.0	1.000	1.232	1.414	1.574	1.721	1.858	1.987
0.1	1.030	1.316	1.538	1.730	1.902	2.062	2.210
0.2	1.035	1.315	1.549	1.756	1.943	2.116	2.279
0.3	1.010	1.269	1.498	1.705	1.896	2.075	2.244
0.4	.9622	1.196	1.411	1.610	1.797	1.975	2.143
0.5	.8996	1.108	1.304	1.491	1.668	1.839	2.003
0.6	.8287	1.012	1.189	1.360	1.525	1.685	1.841
0.7	.7543	.9149	1.073	1.227	1.378	1.526	1.670
0.8	.6799	.8197	.9588	1.097	1.233	1.368	1.501
0.9	.6078	.7290	.8508	.9729	1.095	1.216	1.337
1.0	.5396	.6442	.7505	.8578	.9658	1.074	1.183
1.1	.4762	.5662	.6584	.7523	.8474	.9435	1.040
1.2	.4181	.4954	.5751	.6568	.7400	.8246	.9103
1.3	.3654	.4316	.5003	.5711	.6566	.7178	.7932
1.4	.3181	.3747	.4337	.4948	.5578	.6224	.6885
1.5	.2760	.3242	.3748	.4274	.4819	.5380	.5956
1.6	.2387	.2798	.3230	.3682	.4151	.4637	.5138
1.7	.2058	.2408	.2777	.3163	.3567	.3986	.4419
1.8	.1771	.2069	.2381	.2712	.3058	.3418	.3792
1.9	.1520	.1771	.2038	.2320	.2616	.2926	.3248
2.0	.1301	.1514	.1741	.1981	.2234	.2499	.2775
2.1	.1112	.1293	.1485	.1689	.1904	.2131	.2367
2.2	.0949	.1101	.1264	.1437	.1621	.1814	.2016
2.3	.0809	.0937	.1075	.1222	.1377	.1542	.1714
2.4	.0688	.0796	.0912	.1037	.1169	.1309	.1456
2.5	.0584	.0675	.0774	.0879	.0991	.1109	.1234
2.6	.0496	.0572	.0655	.0744	.0839	.0939	.1046
2.7	.0420	.0485	.0554	.0629	.0709	.0794	.0885
2.8	.0355	.0410	.0468	.0532	.0599	.0671	.0748
2.9	.0300	.0346	.0395	.0449	.0506	.0566	.0631
3.0	.0254	.0292	.0334	.0378	.0426	.0478	.0532

TABLE CI—*continued*

δ	ζ	0.8	1.0	1.2	1.4	1.6	1.8	2.0	2.5	3.0	3.5	4.0	4.5	5.0	5.5	6.0
0.0		2.228	2.451	2.661	2.861	3.051	3.235	3.411	3.831	4.224	4.596	4.951	5.292	5.620	5.936	6.241
0.2		2.579	2.853	3.109	3.350	3.579	3.797	4.006	4.500	4.958	5.388	5.797	6.186	6.560	6.919	7.263
0.4		2.460	2.755	3.031	3.293	3.543	3.783	4.013	4.556	5.060	5.535	5.984	6.413	6.823	7.218	7.596
0.6		2.139	2.422	2.694	2.954	3.204	3.446	3.681	4.238	4.761	5.256	5.727	6.178	6.611	7.028	7.428
0.8		1.761	2.015	2.262	2.502	2.737	2.966	3.190	3.729	4.242	4.733	5.204	5.658	6.097	6.520	6.929
1.0		1.399	1.614	1.828	2.039	2.247	2.453	2.656	3.153	3.634	4.100	4.552	4.991	5.418	5.833	6.237
1.2		1.084	1.260	1.437	1.615	1.793	1.971	2.148	2.587	3.020	3.446	3.865	4.275	4.677	5.072	5.458
1.4		.8243	.9641	1.107	1.252	1.399	1.548	1.697	2.074	2.452	2.829	3.204	3.576	3.944	4.308	4.667
1.6		;6178	.7265	.8391	.9549	1.073	1.194	1.317	1.631	1.952	2.277	2.605	2.933	3.262	3.589	3.914
1.8		.4578	.5409	.6279	.7185	.8121	.9086	1.007	1.264	1.530	1.804	2.083	2.367	2.653	2.941	3.230
2.0		.3361	.3987	.4650	.5347	.6074	.6829	.7610	.9661	1.183	1.409	1.643	1.883	2.127	2.376	2.627
2.2		.2448	.2915	.3414	.3943	.4500	.5083	.5690	.7305	.9041	1.088	1.280	1.479	1.685	1.896	2.110
2.4		.1772	.2117	.2488	.2885	.3306	.3751	.4218	.5473	.6842	.8311	.9868	1.150	1.320	1.496	1.676
2.6		.1275	..1528	.1802	.2097	.2413	.2748	.3102	.4066	.5133	.6293	.7537	.8856	1.024	1.169	1.319
2.8		.0914	.1097	.1298	.1516	.1750	.2001	.2267	.3000	.3822	.4727	.5709	.6761	.7878	.9053	1.028
3.0		.0652	.0784	.0931	.1090	.1263	.1449	.1647	.2199	.2827	.3526	.4293	.5123	6012	.6957	.7952

TABLE CII

Tabulation of $Y(\xi, \delta)$

For $\delta < 0{\cdot}025$, $\xi < 0{\cdot}1$ $\Big\}$ $Y(\xi, \delta) \simeq (1 + \pi\xi) \ln (1{\cdot}12/(\xi + \delta))$

δ \ ξ	0.0	0.1	0.2	0.3	0.4	0.5	0.6
0.0	∞	3.101	2.729	2.551	2.442	2.367	2.311
0.025	3.800						
0.05	3.100	2.589					
0.075	2.687						
0.1	2.392	2.214	2.127	2.073	2.035	2.007	1.986
0.2	1.674	1.679	1.681	1.682	1.683	1.684	1.685
0.3	1.258	1.306	1.340	1.366	1.386	1.403	1.417
0.4	.9738	1.031	1.074	1.110	1.139	1.164	1.186
0.5	.7656	.8201	.8647	.9023	.9346	.9628	.9878
0.6	.6078	.6564	.6980	.7342	.7662	.7947	.8204
0.7	.4856	.5276	.5647	.5978	.6277	.6549	.6797
0.8	.3898	.4254	.4576	.4871	.5141	.5390	.5622
0.9	.3139	.3437	.3714	.3970	.4209	.4433	.4643
1.0	.2534	.2783	.3017	.3237	.3446	.3643	.3830
1.1	.2050	.2256	.2453	.2641	.2820	.2992	.3156
1.2	.1661	.1832	.1996	.2155	.2308	.2456	.2599
1.3	.1348	.1488	.1625	.1759	.1889	.2016	.2139
1.4	.1094	.1210	.1324	.1436	.1546	.1654	.1759
1.5	.0890	.0985	.1079	.1173	.1265	.1356	.1446
1.6	.0724	.0802	.0880	.0958	.1035	.1112	.1188
1.7	.0589	.0653	.0718	.0783	.0847	.0912	.0976
1.8	.0480	.0532	.0586	.0639	.0693	.0748	.0802
1.9	.0391	.0434	.0478	.0522	.0567	.0613	.0658
2.0	.0319	.0354	.0390	.0427	.0464	.0502	.0540
2.1	.0260	.0289	.0319	.0349	.0380	.0411	.0443
2.2	.0212	.0236	.0260	.0285	.0311	.0337	.0364
2.3	.0173	.0192	.0213	.0233	.0255	.0276	.0298
2.4	.0141	.0157	.0174	.0191	.0208	.0226	.0245
2.5	.0115	.0123	.0142	.0156	.0170	.0185	.0201
2.6	.0094	.0105	.0116	.0128	.0140	.0152	.0165
2.7	.0077	.0086	.0095	.0104	.0114	.0124	.0135
2.8	.0063	.0070	.0077	.0085	.0093	.0102	.0111
2.9	.0051	.0057	.0063	.0070	.0076	.0083	.0091
3.0	.0042	.0047	.0052	.0057	.0063	.0068	.0074

TABLE CII—*continued*

δ	ξ 0.8	1.0	1.2	1.4	1.6	1.8	2.0	2.5	3.0	3.5	4.0	4.5	5.0	5.5	6.0
0.0	2.233	2.180	2.141	2.111	2.087	2.068	2.052	2.020	1.997	1.980	1.966	1.955	1.945	1.937	1.929
0.2	1.686	1.687	1.688	1.689	1.691	1.692	1.693	1.695	1.697	1.699	1.701	1.703	1.704	1.705	1.705
0.4	1.222	1.250	1.274	1.294	1.312	1.327	1.340	1.369	1.391	1.409	1.425	1.438	1.450	1.460	1.468
0.6	.8649	.9025	.9349	.9632	.9882	1.011	1.031	1.074	1.109	1.138	1.163	1.185	1.204	1.221	1.236
0.8	.6039	.6405	.6731	.7024	.7209	.7532	.7754	.8239	.8647	.8995	.9299	.9567	.9804	1.002	1.021
1.0	.4177	.4493	.4782	.5047	.5293	.5522	.5735	.6212	.6624	.6984	.7304	.7591	.7849	.8083	.8294
1.2	.2871	.3125	.3363	.3587	.3798	.3997	.4186	.4617	.5000	.5343	.5653	.5935	.6193	.6430	.6646
1.4	.1964	.2159	.2347	.2527	.2699	.2864	.3022	.3392	.3729	.4037	.4320	.4582	.4824	.5050	.5259
1.6	.1339	.1485	.1628	.1768	.1903	.2035	.2163	.2468	.2752	.3017	.3265	.3498	.3717	.3923	.4116
1.8	.0910	.1018	.1125	.1230	.1334	.1436	.1537	.1780	.2013	.2234	.2444	.2645	.2836	.3017	.3190
2.0	.0617	.0695	.0774	.0852	.0930	.1008	.1085	.1276	.1461	.1641	.1815	.1983	.2144	.2301	.2450
2.2	.0418	.0474	.0531	.0588	.0646	.0704	.0762	.0908	.1054	.1197	.1337	.1475	.1609	.1740	.1867
2.4	.0283	.0322	.0363	.0404	.0447	.0490	.0533	.0644	.0755	.0867	.0979	.1090	.1199	.1307	.1413
2.6	.0191	.0219	.0248	.0277	.0308	.0339	.0371	.0454	.0539	.0625	.0712	.0800	.0888	.0975	.1062
2.8	.0129	.0148	.0169	.0190	.0212	.0235	.0258	.0319	.0382	.0448	.0516	.0584	.0653	.0723	.0793
3.0	.0087	.0101	.0115	.0130	.0145	.0162	.0179	.0223	.0270	.0320	.0371	.0424	.0478	.0533	.0589

where R_1 is the impact parameter corresponding to the closest approach R_1^c. Therefore in weak coupling

$$Q_{n\to n'}{}^{W} = \frac{I_H}{W_n}\left[8\left(\frac{I_H}{\Delta E_{nn'}} f_{n\to n'}\right) Y(\xi, \delta_0)\right] \tag{C14}$$

where $\delta_0 = R_0^c|k_n - k_{n'}|$ and R_0^c is the smaller of the mean atomic radii in states n and n'. In strong coupling

$$Q_{n\to n'}{}^{S} = \frac{I_H}{W_n}\left[8\left(\frac{I_H}{\Delta E_{n'n}} f_{n\to n'}\right) Y(\xi, \delta_1) + \frac{Z}{a_0} R_1^c + \tfrac{1}{2} k_n k_{n'} (R_1^c)^2\right] \pi a_0^2 \tag{C15}$$

and

$$Y(\xi, \delta_1) = [\exp(\pi\xi)\, K_{i\xi}(\xi\epsilon)\, K_{i\xi}'(\xi\epsilon)(\xi\epsilon)]1_{(\xi\epsilon)1}.$$

The functions X and Y are tabulated in Tables CI and CII.

In entirely analogous fashion the proton impact cross-sections can be obtained, whereupon it is found that

$$\begin{aligned} X(-\xi, \delta) &= \exp(-2\pi\xi)\, X(\xi, \delta - 2\xi) \\ Y(-\xi, \delta) &= \exp(-2\pi\xi)\, Y(\xi, \delta - 2\xi). \end{aligned} \tag{C16}$$

The formulae for X and Y apply for $W_> \geq 1{\cdot}25\ \Delta E_{nn'}$ (where $W_>$ is the greater of W_n and $W_{n'}$). Then for $W_> < 1{\cdot}25\ \Delta E_{nn'}$, we approximate by

$$W_> Q(W_>) = 1{\cdot}25\ C\ \Delta E_{nn'} Q(1{\cdot}25\ \Delta E_{nn'})$$

where

$$C = \begin{cases} \sqrt{\dfrac{4W_<}{\Delta E_{nn'}}} & \text{for electron and proton collisions with neutral targets} \\ 1 & \text{for electron collisions with ion targets} \\ \exp\left\{\pi Z \sqrt{\dfrac{mI_H}{m_e}}\left[\dfrac{1{\cdot}1056}{\sqrt{\Delta E_{nn'}}} - \dfrac{\Delta E_{nn'}}{W_>\sqrt{W_<} + W_<\sqrt{W_>}}\right]\right\} & \text{for protons with ion targets.} \end{cases}$$